

Introduction to Astrophysics and Cosmology

Star Formation

An introduction to modern Astrophysics chapter 12

Helga Dénés 2025 S1 Yachay Tech
hdenes@yachaytech.edu.ec



**SCHOOL OF
PHYSICAL SCIENCES
AND NANOTECHNOLOGY**

Numerical Simulations of Protostellar Evolution

To investigate the nature of the gravitational collapse of a cloud in detail, we must solve the magnetohydrodynamic equations numerically. Limits in computing power and numerical methods still necessitate making numerous and significant simplifying assumptions.

- Consider a **spherical cloud of approximately $1 M_{\odot}$** and solar composition that is supercritical.
- Initially the early stages of the free-fall collapse are nearly **isothermal** because light near the center of the collapse can travel significant distances before being absorbed by dust.
- Due to an initial slight increase in density toward the center of the cloud, the free-fall timescale is shorter near the center and the density increases more rapidly there (**inside-out collapse**).
- When the density of the material near the center of the collapse region reaches approximately $10^{-10} \text{ kg m}^{-3}$, the region becomes optically thick and the **collapse becomes more adiabatic**. The opacity of the cloud at this point is primarily due to the presence of dust.
- The increased pressure substantially **slows the rate of collapse** near the core.
- At this point the central region is **nearly in hydrostatic equilibrium** with a radius of approximately 5 AU. It is this central object that is referred to as a **protostar**.

Numerical Simulations of Protostellar Evolution

Protostar IC 2631

One observable consequence of the cloud becoming **optically thick** is that the gravitational potential energy being released during the collapse is converted into heat and then radiated away in the infrared as **blackbody radiation**.

By computing the rate of **energy release (the luminosity)** and the radius of the cloud where the optical depth is $\tau = 2/3$, the **effective temperature may be determined** using the following equation:

$$L = 4\pi R^2 \sigma T_e^4$$

With the identification of a photosphere, it becomes possible to plot the location of the simulated cloud on the H–R diagram as a function of time.



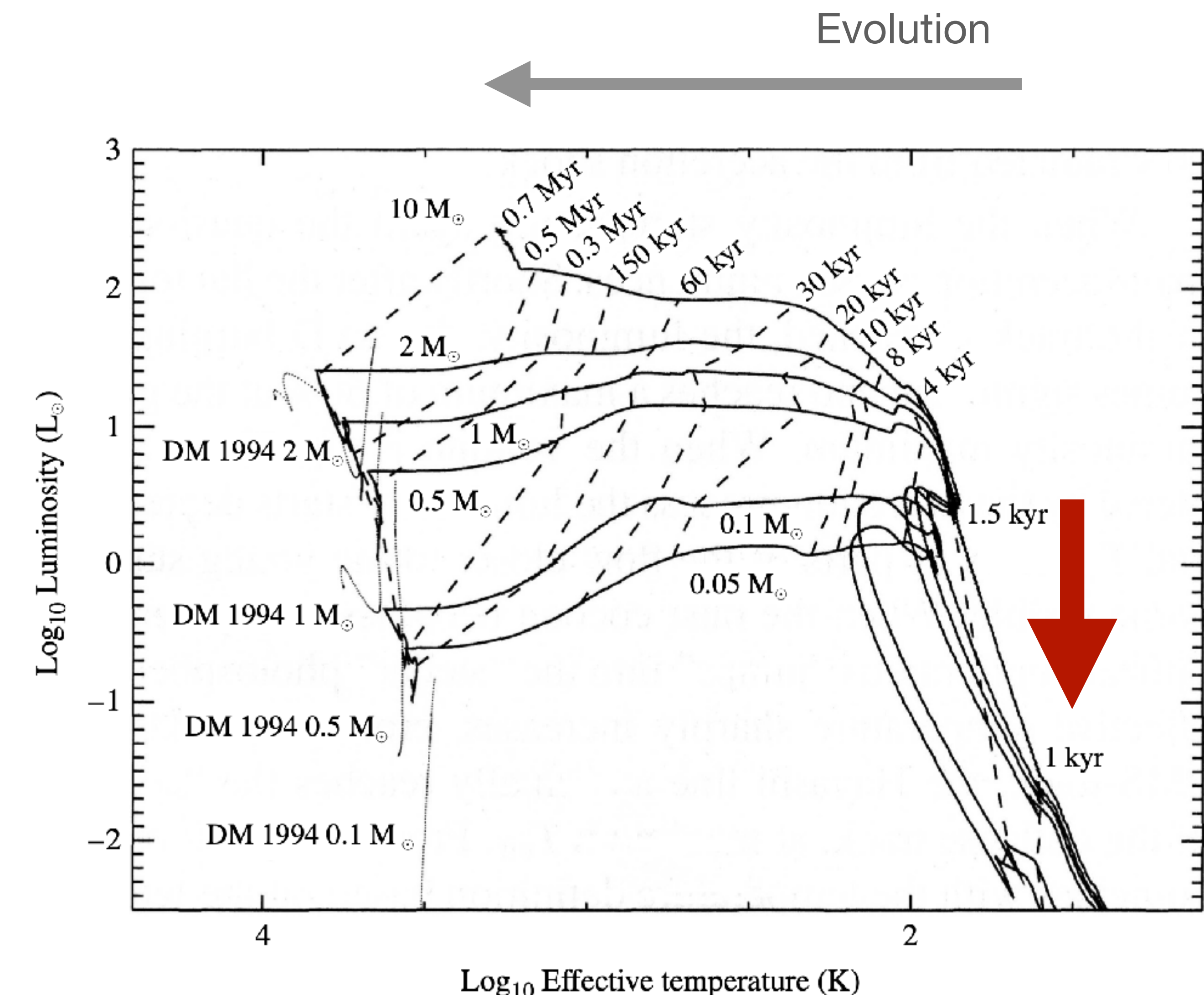
Numerical Simulations of Protostellar Evolution

Curves that depict the life histories of stars on the H–R diagram are known as **evolutionary tracks**.

The Figure shows **theoretical evolutionary tracks** of $0.05, 0.1, 0.5, 1, 2$, and $10 M_{\odot}$ clouds computed through the protostar phase.

As the collapse continues to accelerate during the **early stages, the luminosity of the protostar increases along with its effective temperature**.

The dashed lines show the **times since collapse began**.



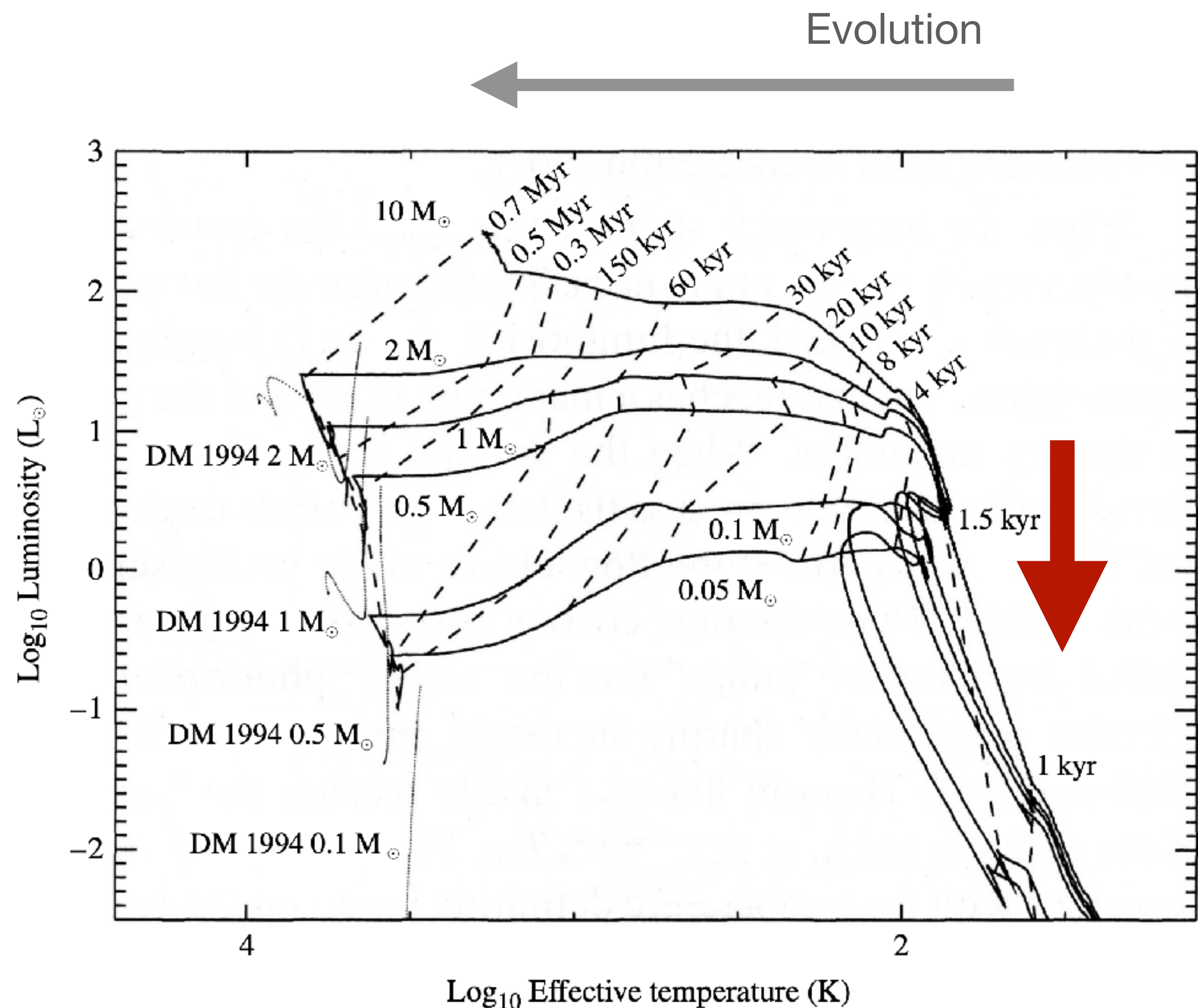
Numerical Simulations of Protostellar Evolution

When the **infalling material** meets the nearly hydrostatic **core**, a **shock wave develops** where the speed of the material exceeds the local sound speed (the material is supersonic). It is at this shock front that the infalling material loses a significant fraction of its kinetic energy in the form of **heat** that “powers” the cloud and produces much of its luminosity.

When the temperature reaches approximately **1000 K** the **dust** within the developing protostar begins to **vaporize** and the **opacity drops**.

Eventually the **temperature becomes high enough** (approximately 2000 K) to cause the **molecular hydrogen to dissociate** into atoms.

This process **absorbs energy** and breaks the hydrostatic equilibrium. As a result, the **core becomes dynamically unstable** and a second **collapse occurs**.



Numerical Simulations of Protostellar Evolution

After this hydrostatic **equilibrium** is re-established.

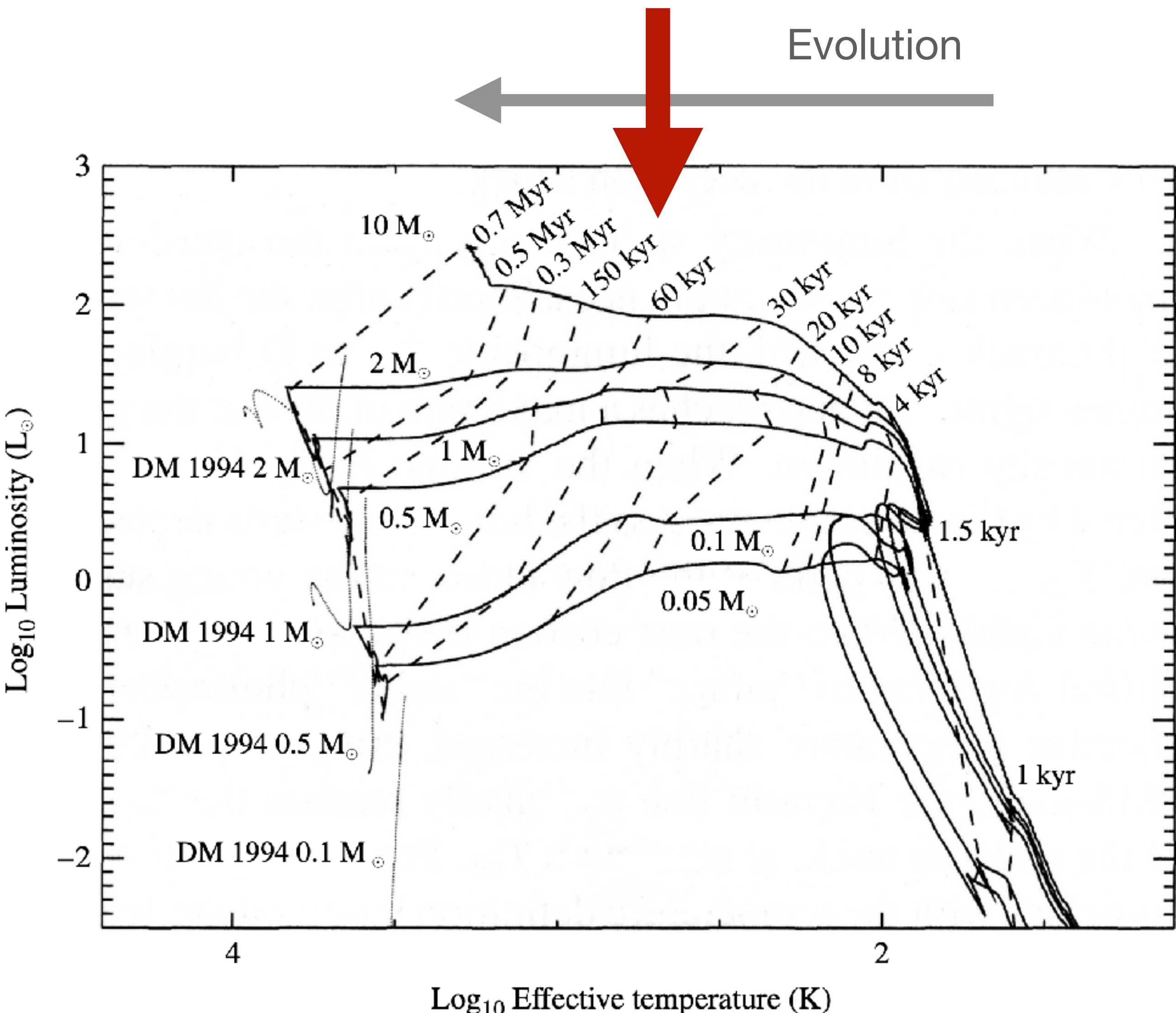
At this point, the core mass is still much less than its final value, implying that **accretion** is still ongoing.

When the **nearly flat, roughly constant luminosity part** of the evolutionary track is reached in the Figure, accretion has settled into a **quasi-steady main accretion phase**.

At about the same time, **temperatures in the deep interior of the protostar have increased enough that deuterium (^2H) begins to burn** (this can happen at relatively low temperatures), producing up to 60% of the luminosity of the 1 M_\odot protostar.

When **deuterium burn-out** occurs, the evolutionary track **bends sharply downward** and the **effective temperature decreases slightly**.

The evolution has now reached a **quasi-static premain-sequence phase**.



Numerical Simulations of Protostellar Evolution

Protostar L1527

Observational verification: Since the collapse should occur deep within a molecular cloud, the protostar itself would likely be **shielded** from direct view by a cocoon of dust.

Consequently, any observational evidence of the collapse would be in the form of small **infrared sources embedded within dense cores or Bok globules**. The detection of protostellar collapse is made more difficult by the relatively small value for the free-fall time, meaning that protostars are **fairly short-lived** objects.

The search for protostars is under way in infrared and millimeter wavelengths.

Some examples:

- B335, a Bok globule in the constellation of Aquila,
- L1527 in Taurus.



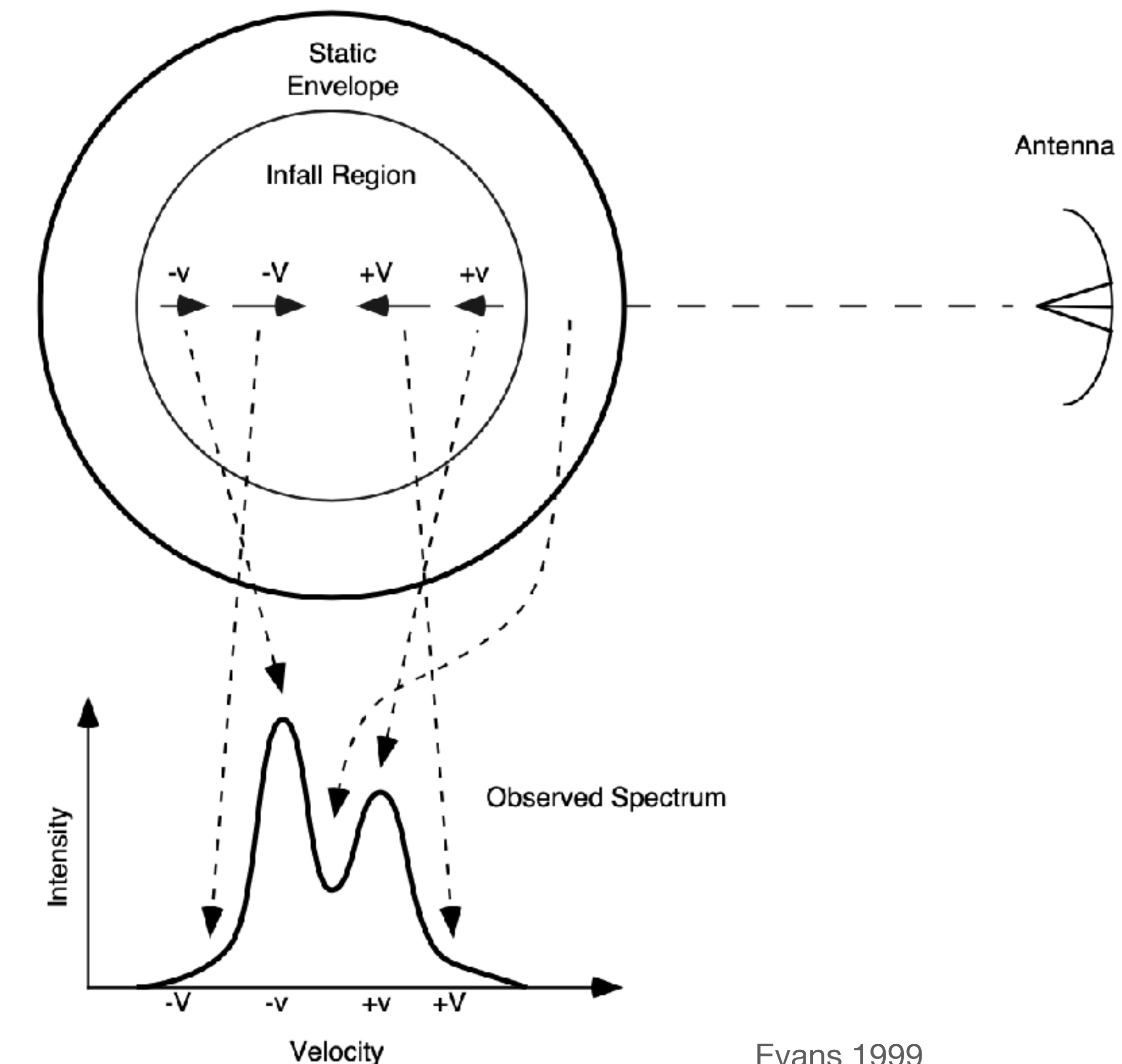
Numerical Simulations of Protostellar Evolution

Studying the details of the infrared spectra of these sources, they have been able to identify possible spectral **signatures of infalling dust and gas** around the embedded infrared objects.

These features involve **Doppler-shifted** sub-structures in the profiles of spectral lines.

For an optically thick line, a central absorption feature is often visible (see Figure). The source of the absorption feature is cool material between the observer and the source of the line (the hotter central region).

The **broad wings** of the line result from Doppler-shifted light coming from **infalling gas**. The blueshifted wing is from infalling gas on the far side of the cloud (therefore moving toward the observer), and the redshifted wing is from infalling gas on the near side of the cloud. Infall has been identified in starless dense cores as well.



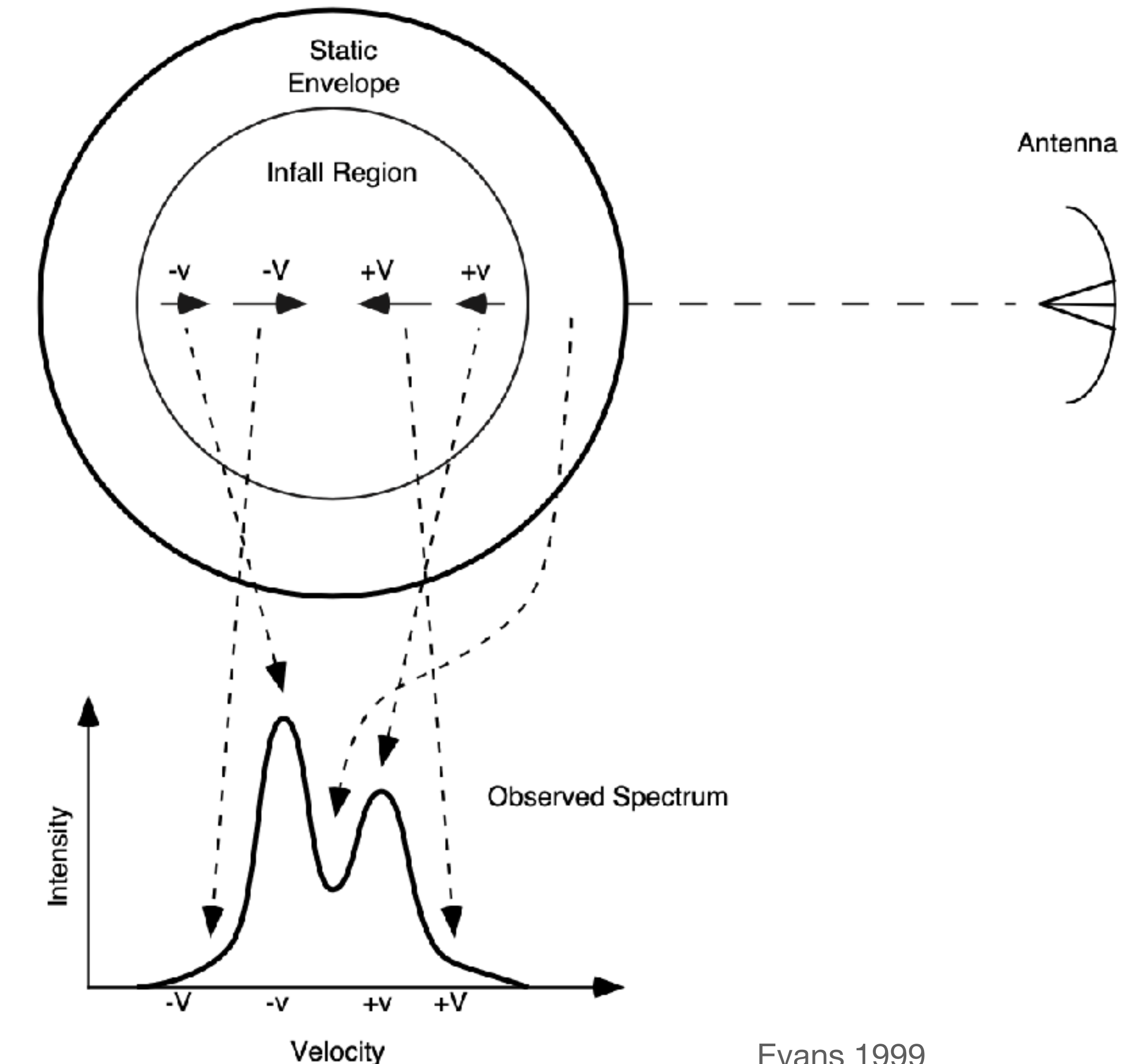
Numerical Simulations of Protostellar Evolution

Once the collapse of a molecular cloud has begun, it is characterized by the free-fall timescale.

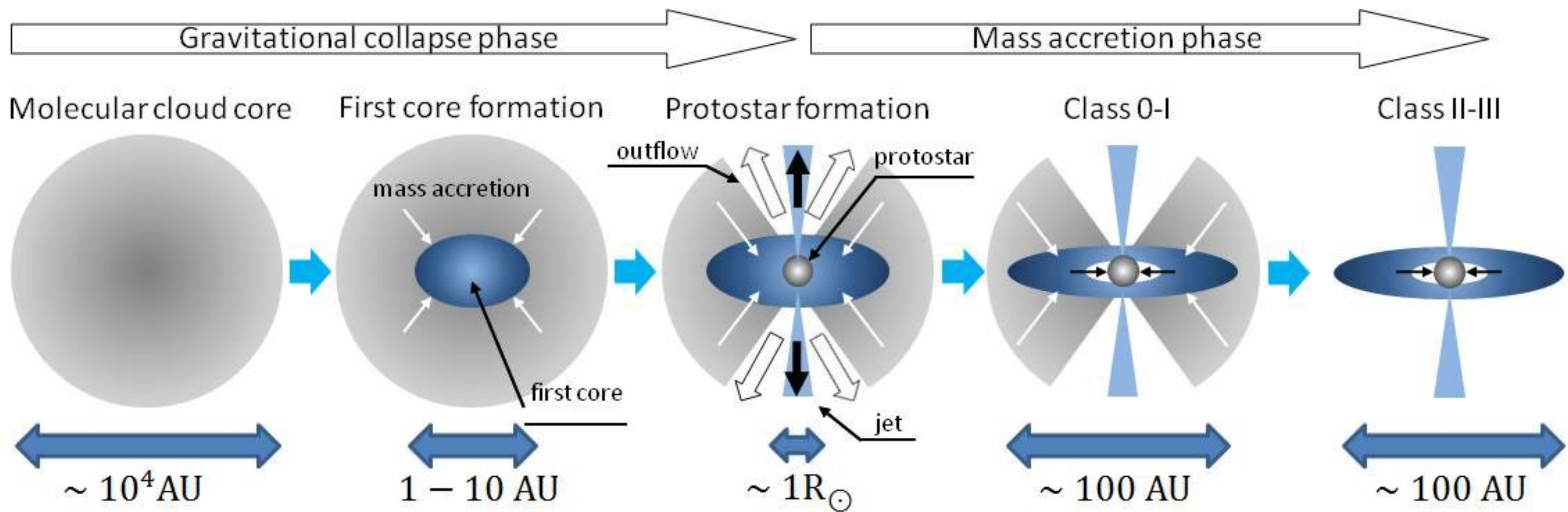
With the formation of a quasi-static protostar, the rate of evolution becomes controlled by the rate at which the star can thermally adjust to the collapse.

This is just the Kelvin–Helmholtz timescale; the gravitational potential energy liberated by the collapse is released over time and is the source of the object’s luminosity.

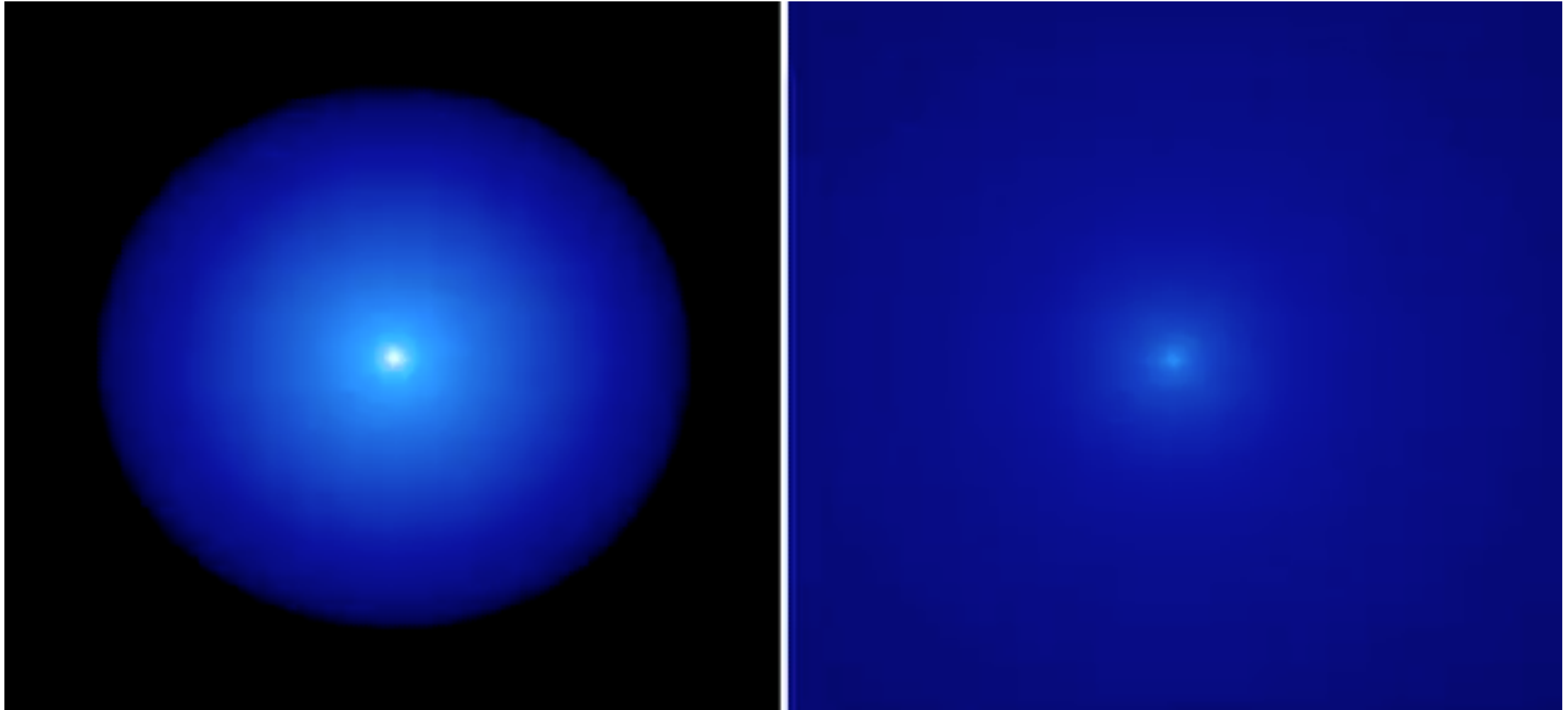
Since $t_{\text{KH}} \gg t_{\text{ff}}$, **protostellar evolution proceeds at a much slower rate than free-fall collapse**. For instance, a $1 M_{\odot}$ star requires almost 40 Myr to contract quasi-statically to its main-sequence structure.



Numerical Simulations of Protostellar Evolution



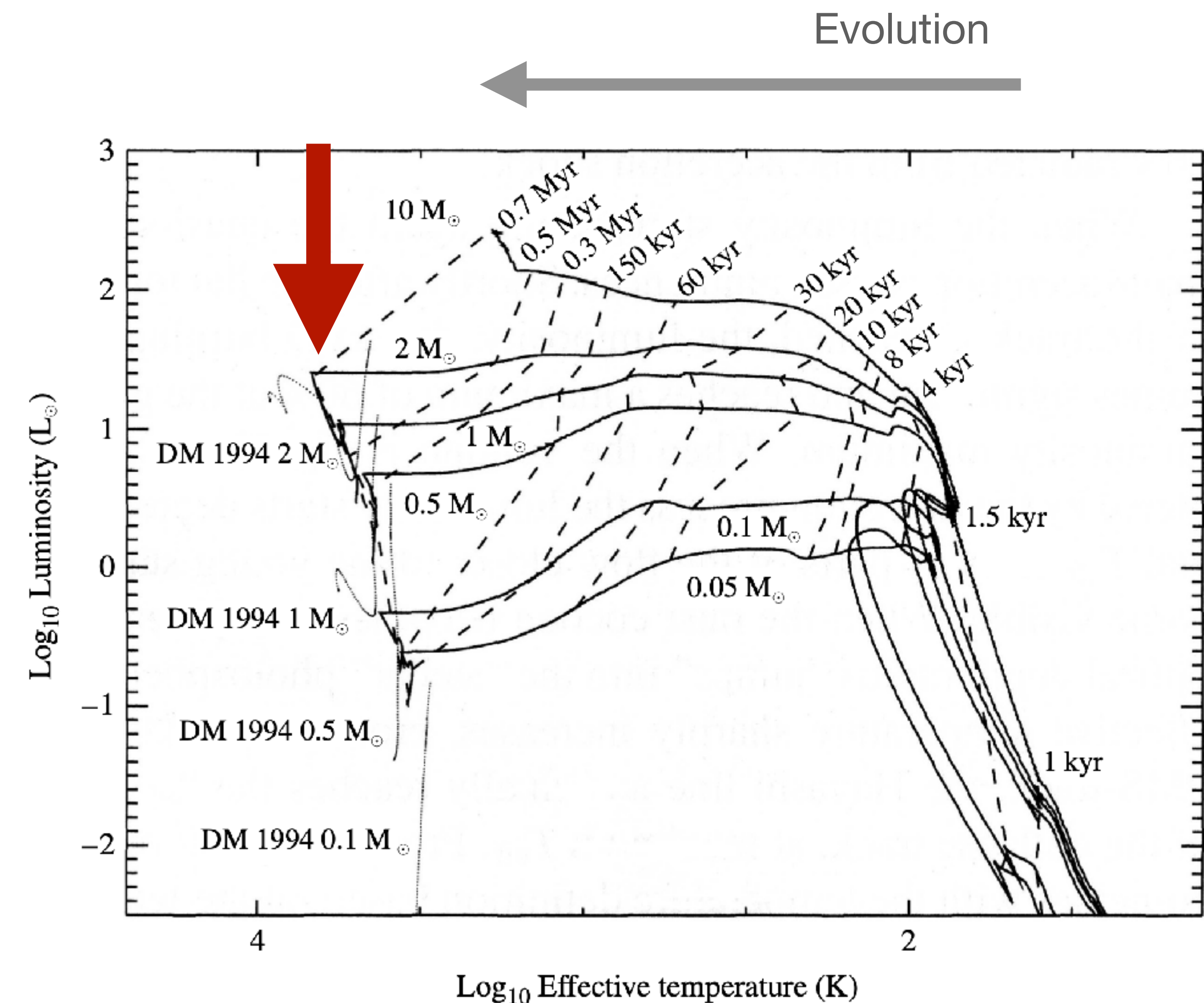
Formation of a Massive protostar



The Hayashi Track

With the steadily increasing effective temperature of the protostar, the opacity of the outer layers becomes dominated by the H^- ion, the extra electrons coming from the partial ionization of some of the heavier elements in the gas that have lower ionization potentials.

As with the envelope of the main-sequence Sun, this large opacity contribution causes the envelope of a contracting protostar to become convective. In some cases the convection zone extends all the way to the center of the star. In 1961, C. Hayashi demonstrated that because of the constraints convection puts on the structure of a star, a deep convective envelope limits its quasi-static evolutionary path to a line that is nearly vertical in the H–R diagram.



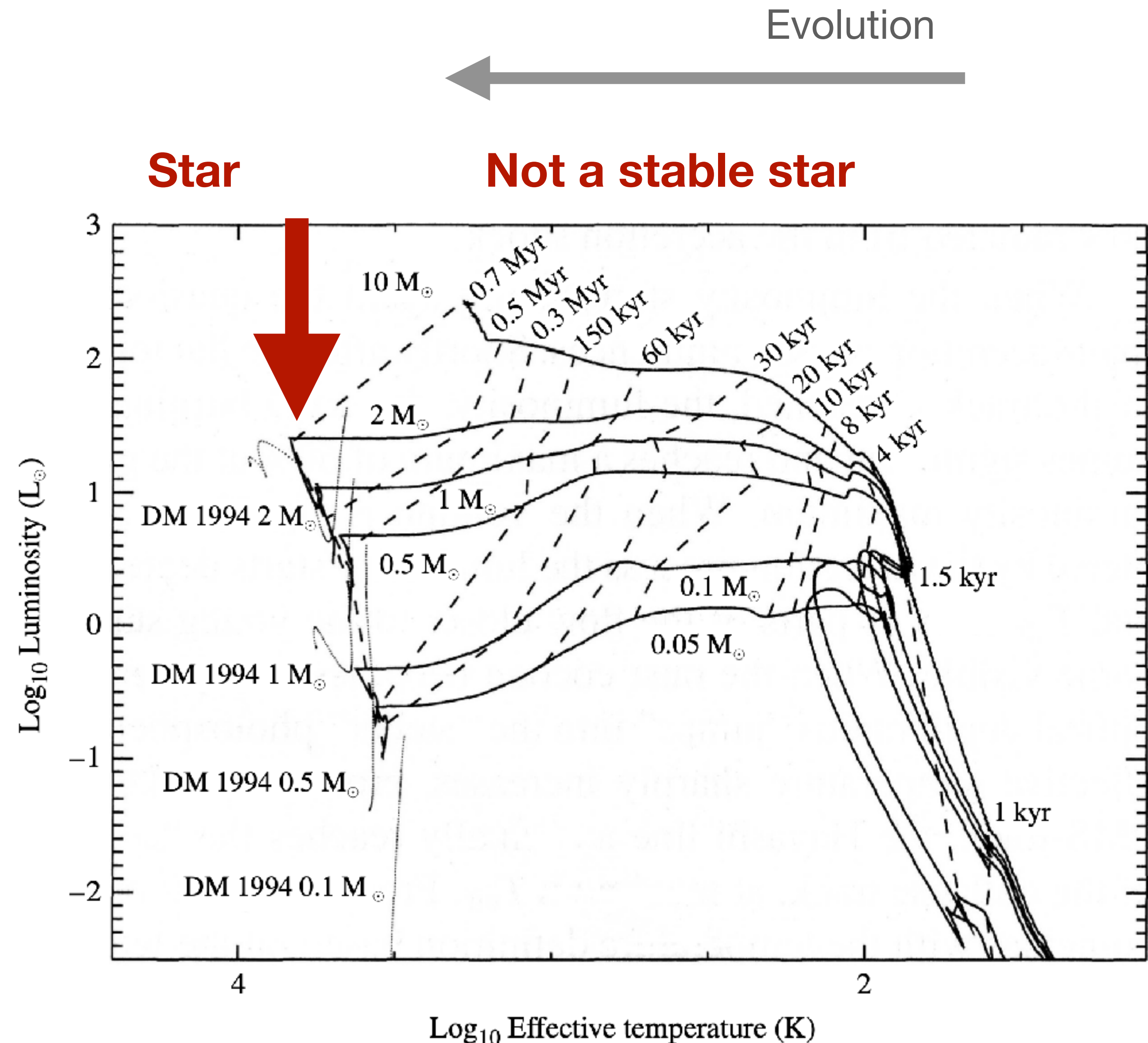
The Hayashi Track

Consequently, as the protostar collapse slows, its luminosity decreases while its effective temperature increases slightly. It is this evolution along the **Hayashi track** that appears as the downward turn at the end of the evolutionary tracks shown in the Figure.

The Hayashi track actually represents a **boundary between “allowed” hydrostatic stellar models and those that are “forbidden.”**

To the **right** of the Hayashi track, there is no mechanism that can adequately transport the luminosity out of the star at those low effective temperatures; hence **no stable stars** can exist there.

To the **left** of the Hayashi track, **convection and/or radiation** is responsible for the necessary energy transport.

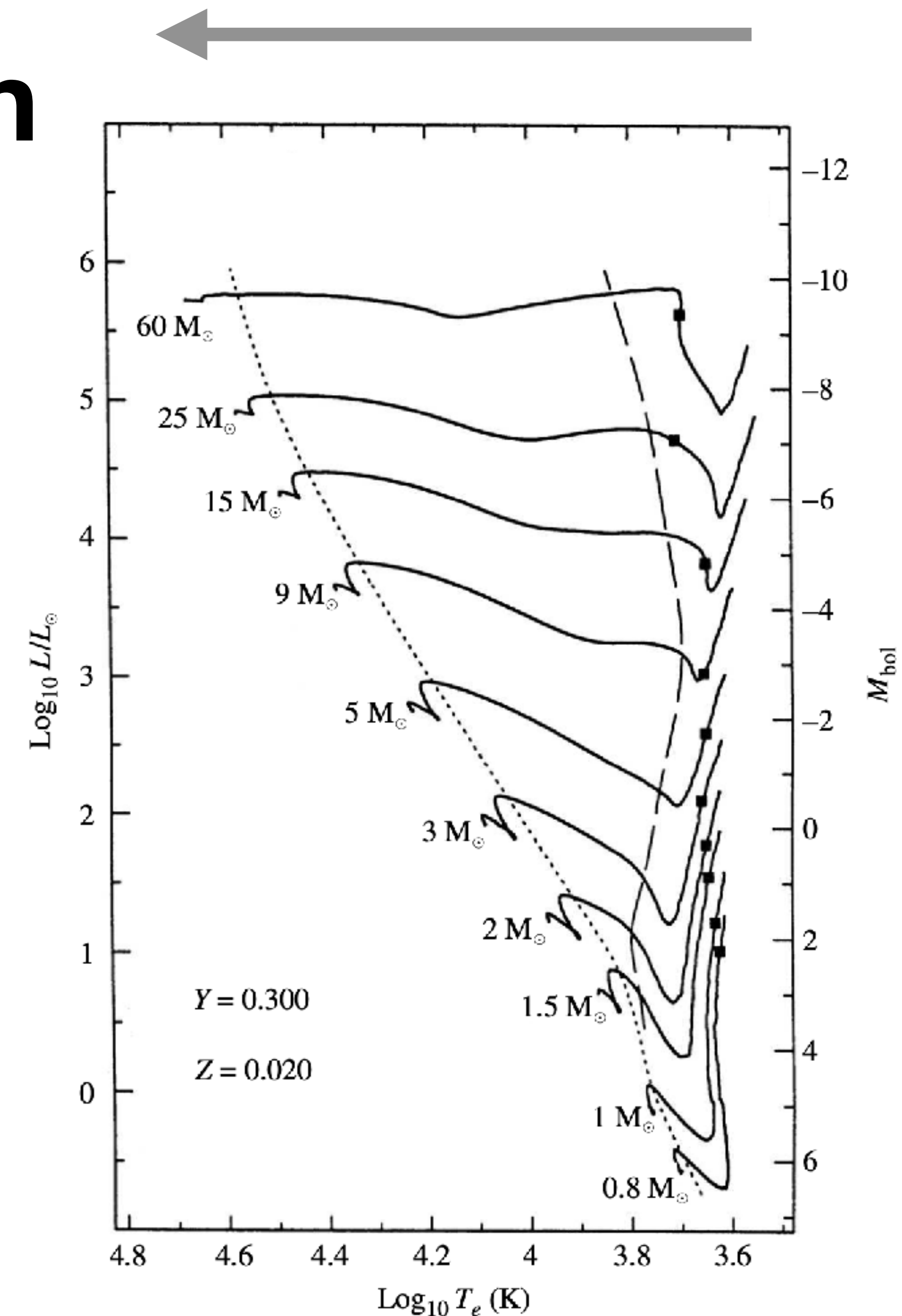


Pre-Main-Sequence evolution

Pre-main-sequence evolutionary tracks can be computed by starting on the Hayashi track. The **pre-main-sequence evolutionary tracks** for a sequence of masses computed with state-of-the-art physics are shown in Fig. 11, and the total time for each evolutionary track is given in Table 1.

TABLE 1 Pre-main-sequence contraction times for the classical models presented in Fig. 11. (Data from Bernasconi and Maeder, *Astron. Astrophys.*, 307, 829, 1996.)

	Initial Mass (M_{\odot})	Contraction Time (Myr)
very fast	60	0.0282
	25	0.0708
	15	0.117
	9	0.288
	5	1.15
	3	7.24
	2	23.4
	1.5	35.4
	1	38.9
	0.8	68.4
Relatively slow		



Pre-Main-Sequence evolution

HBC 1 is a young pre-main-sequence star

HBC 1 illuminates a wispy reflection nebula known as IRAS 00044+6521. Formed from clouds of interstellar dust, reflection nebulae do not emit any visible light of their own and instead — like fog encompassing a lamppost — shine via the light from the stars embedded within.

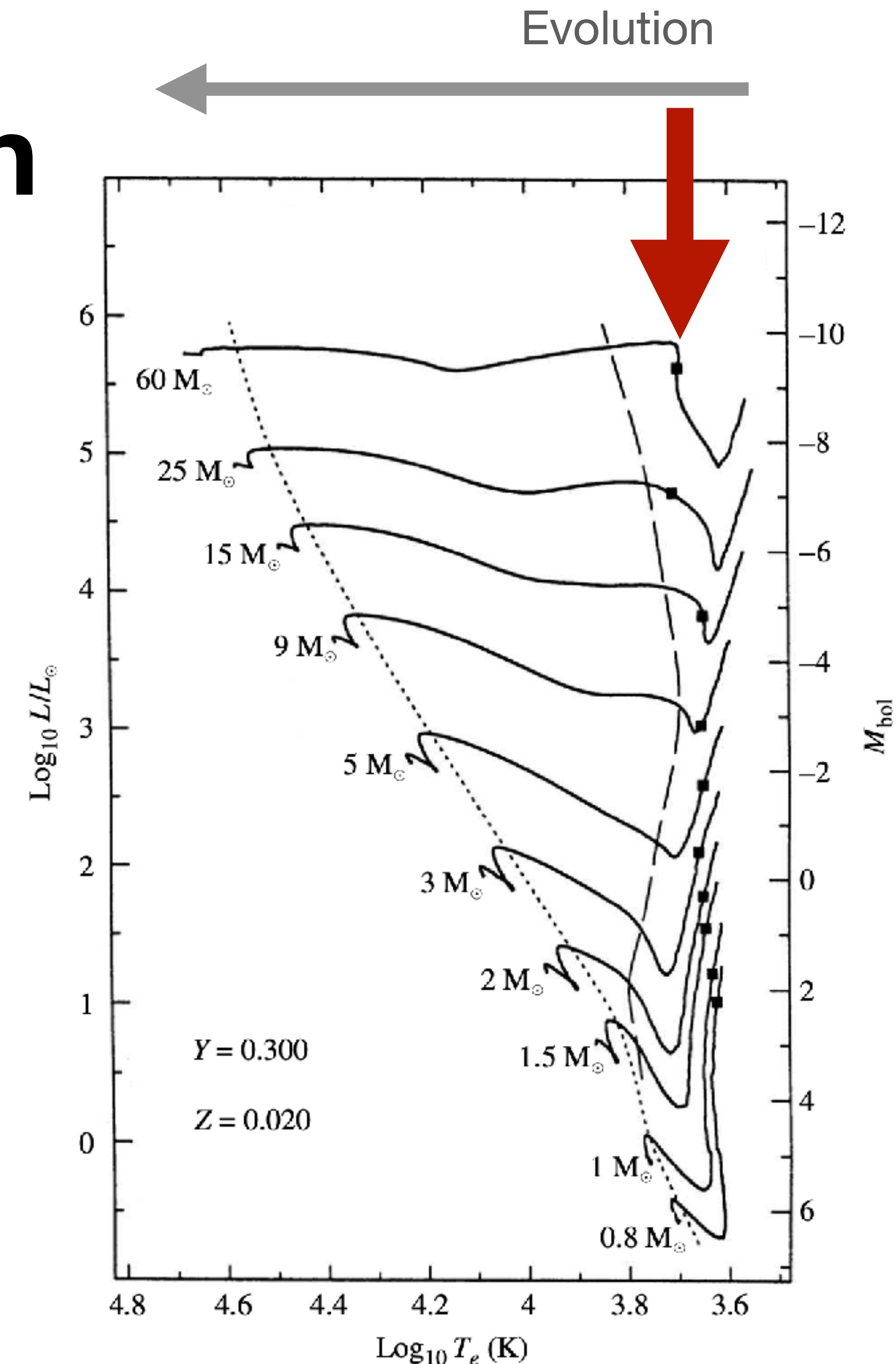


Pre-Main-Sequence evolution

Consider the pre-main-sequence evolution of a $1 M_{\odot}$ star, beginning on the Hayashi track.

With the high H^- opacity near the surface, the **star is completely convective during approximately the first one million years of the collapse**. In these models, **deuterium burning** also occurs during this early period of collapse, beginning at the square indicated on the evolutionary tracks in the Figure.

However, since 2H is not very abundant, the **nuclear reactions** have little effect on the overall collapse; they simply **slow the rate of collapse slightly**.

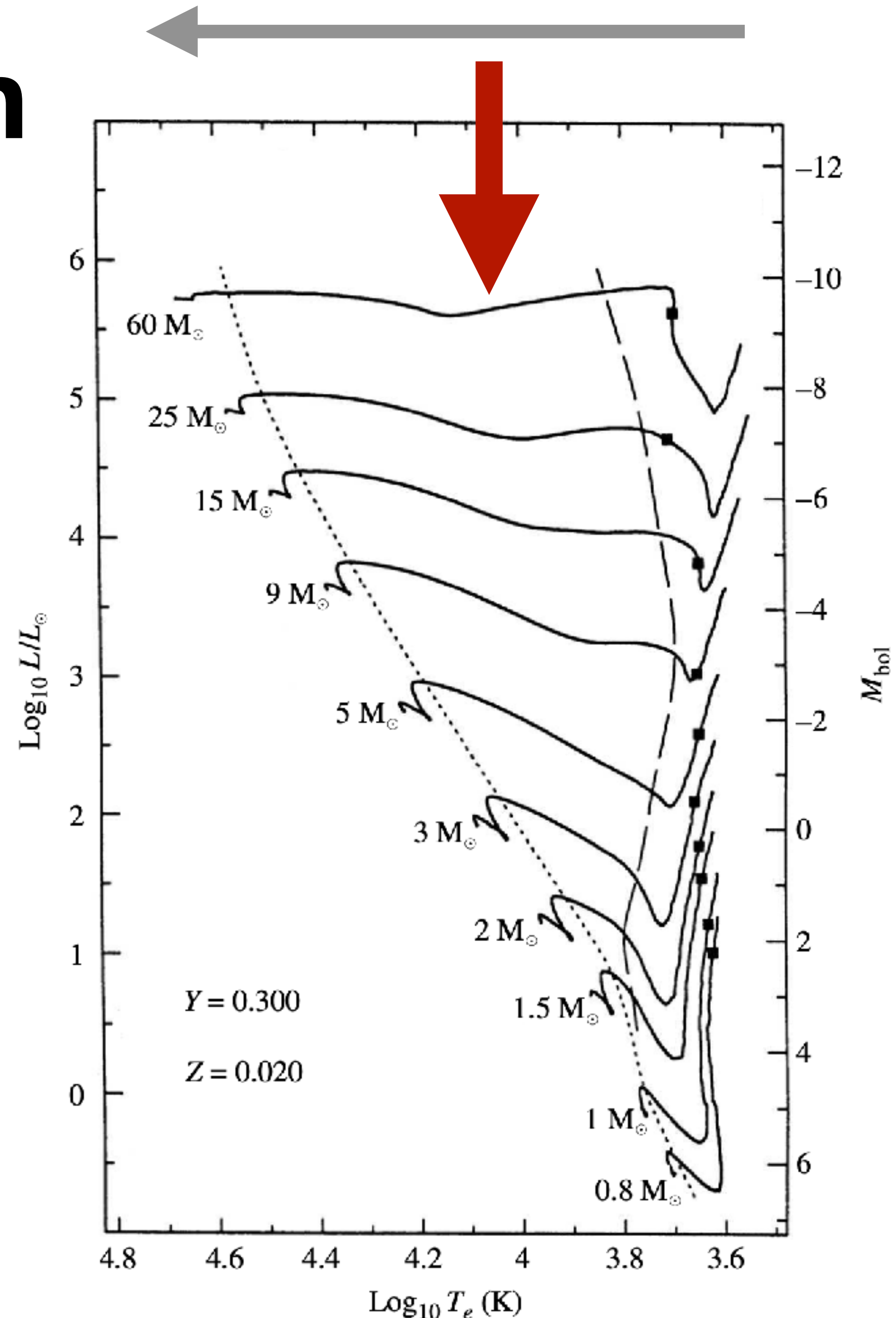


Evolution

Pre-Main-Sequence evolution

As the **central temperature continues to rise**, increasing levels of ionization decrease the opacity in that region and a **radiative core develops**, progressively encompassing more and more of the star's mass.

At the point of **minimum luminosity in the tracks**, the existence of the radiative core allows energy to escape into the convective envelope more readily, causing the luminosity of the star to increase again. Also, the effective temperature continues to increase, since the star is still shrinking.



Evolution

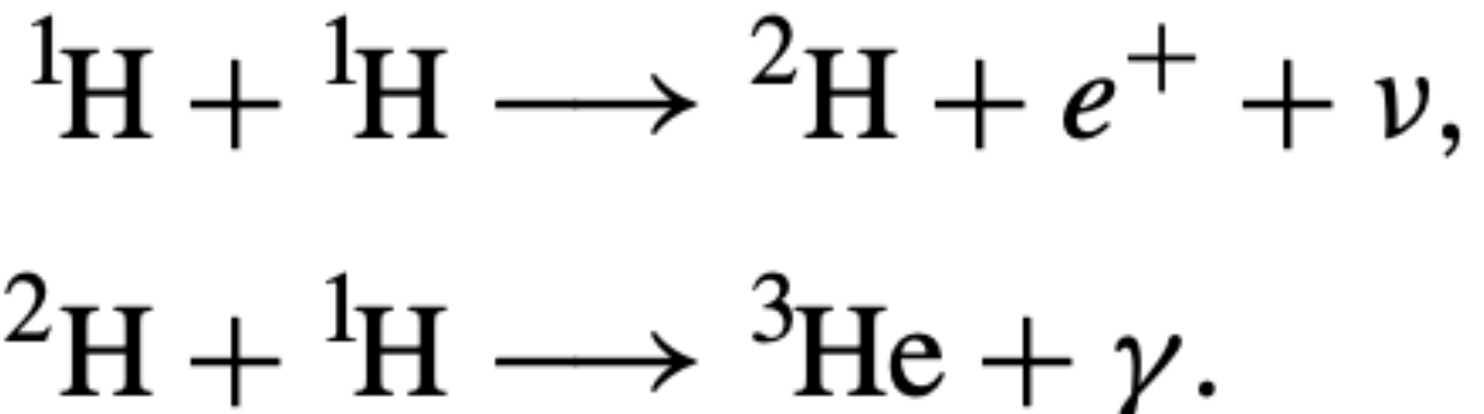
Pre-Main-Sequence evolution

At about the time that the luminosity begins to increase again, the **temperature near the center has become high enough for nuclear reactions to begin** in full, although not yet at their equilibrium rates.

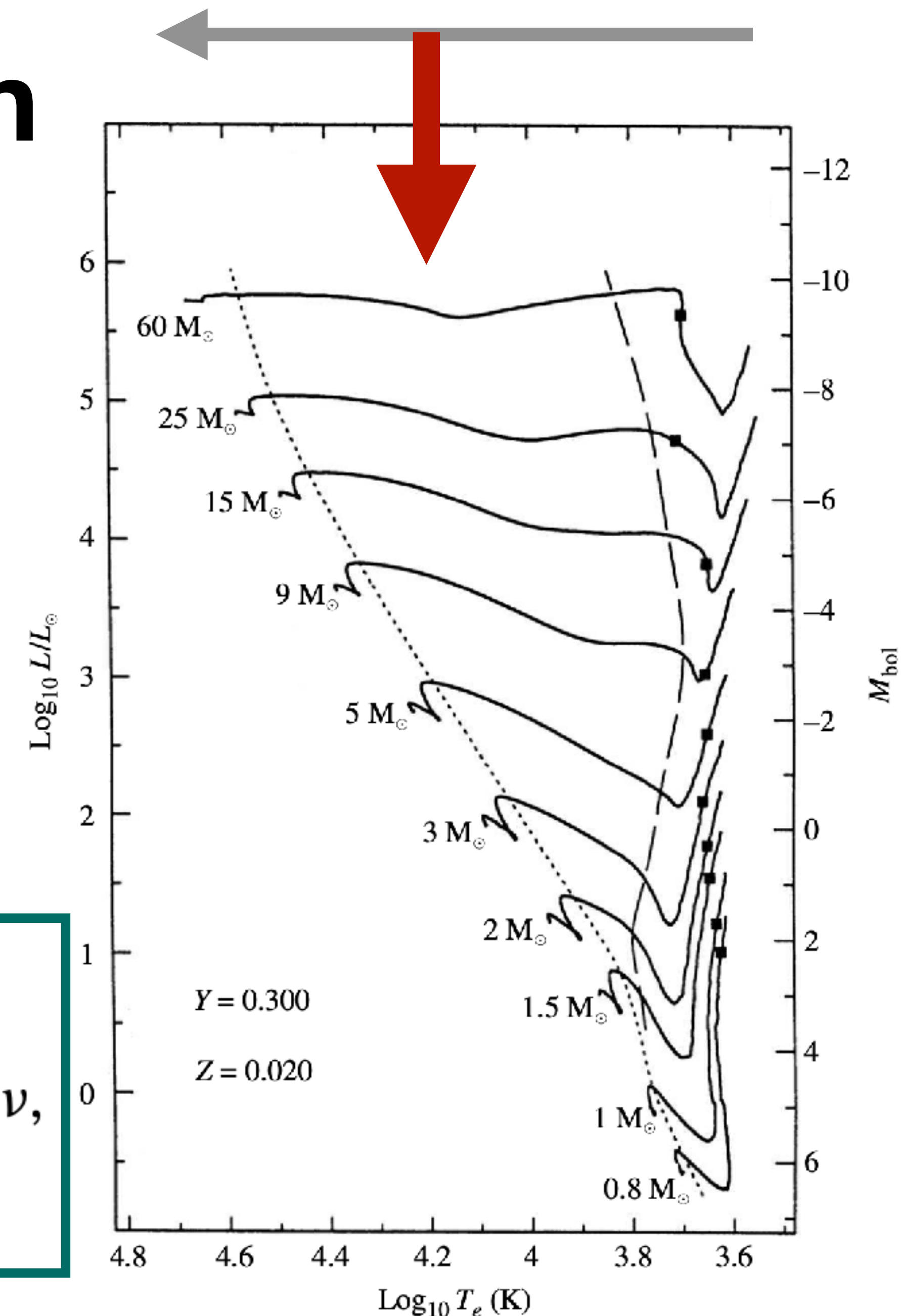
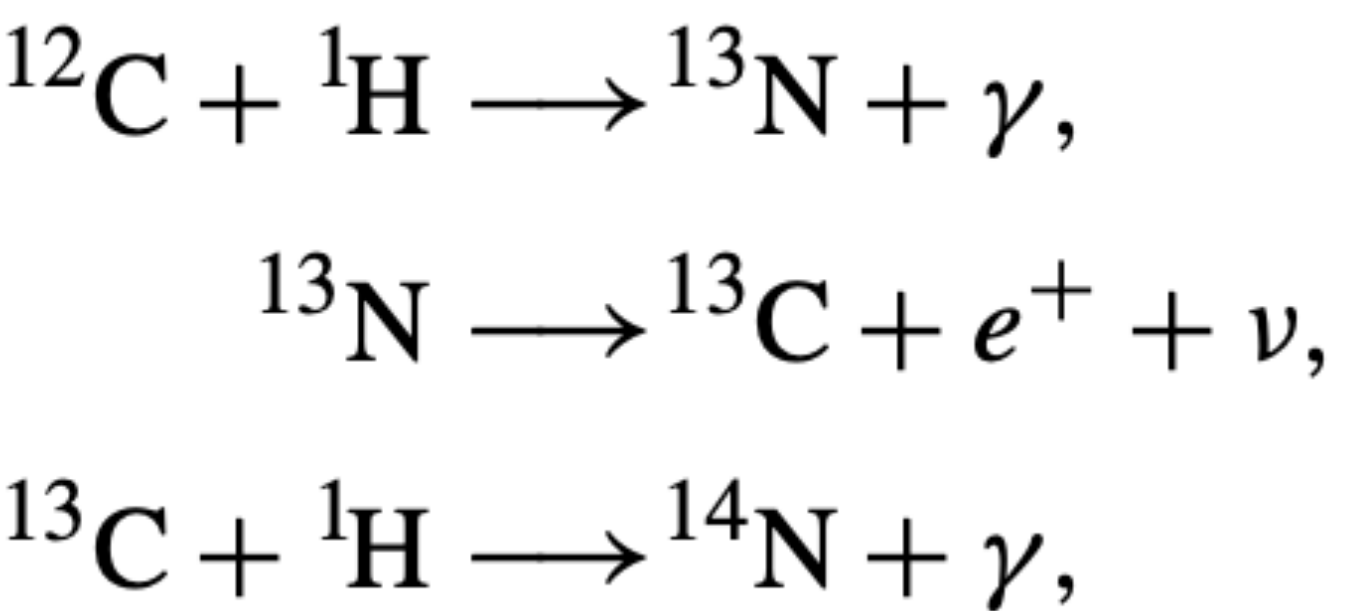
Initially, the first two steps of the PP I chain [^1H to ^3He] and the CNO reactions [^{12}C into ^{14}N] dominate the nuclear energy production.

With time, these **reactions provide an increasingly larger fraction of the luminosity**, while the energy production due to gravitational collapse makes less of a contribution to L.

PP chain



CNO cycle

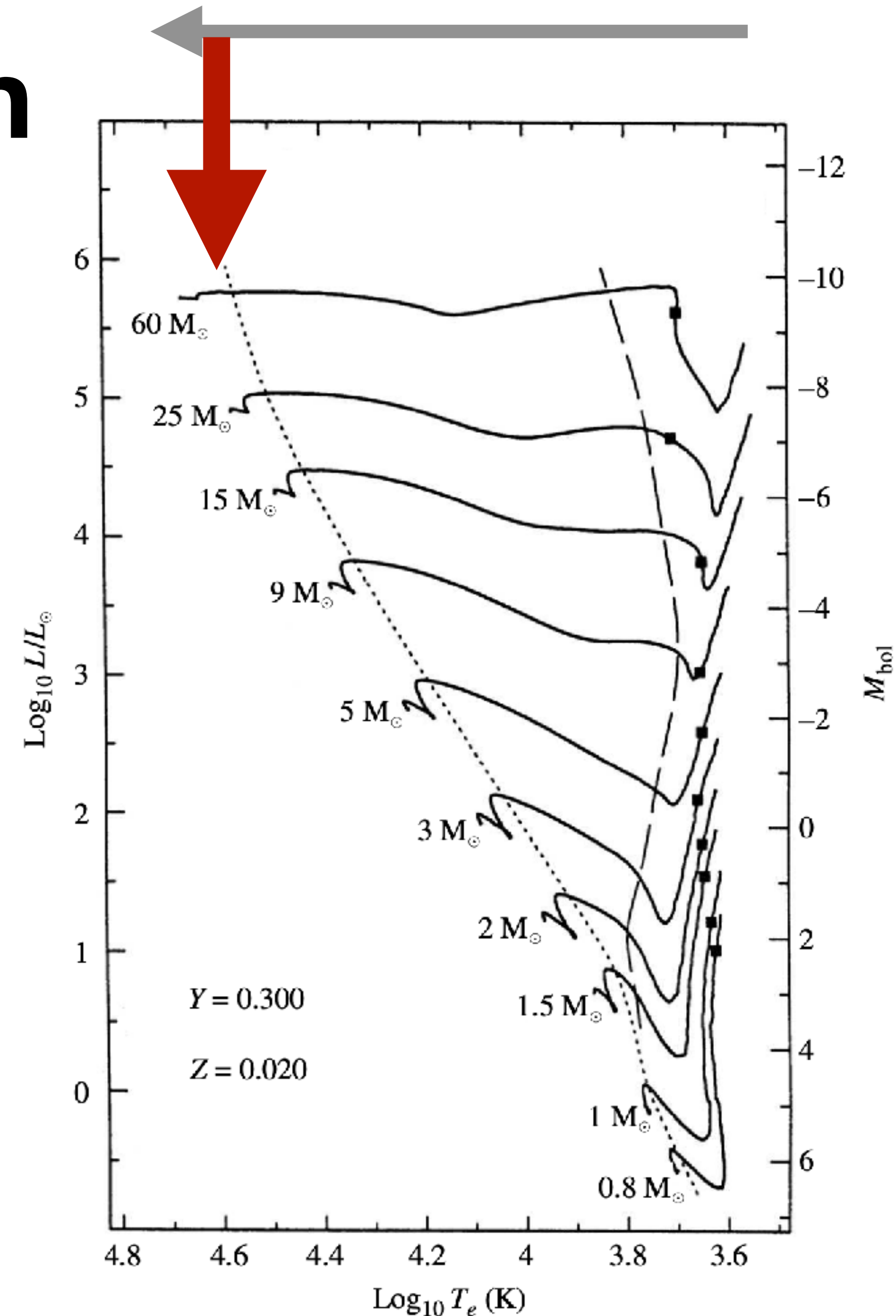


Pre-Main-Sequence evolution

Due to the onset of the highly temperature-dependent **CNO reactions**, a **steep temperature gradient** is established in the core, and some convection again develops in that region.

At the local maximum in the luminosity on the H–R diagram near the short dashed line, the rate of **nuclear energy production** has become so great that the central **core is forced to expand** somewhat, causing the gravitational energy term to become negative.

This effect is apparent **at the surface as the total luminosity decreases** toward its main-sequence value, accompanied by a **decrease in the effective temperature**.

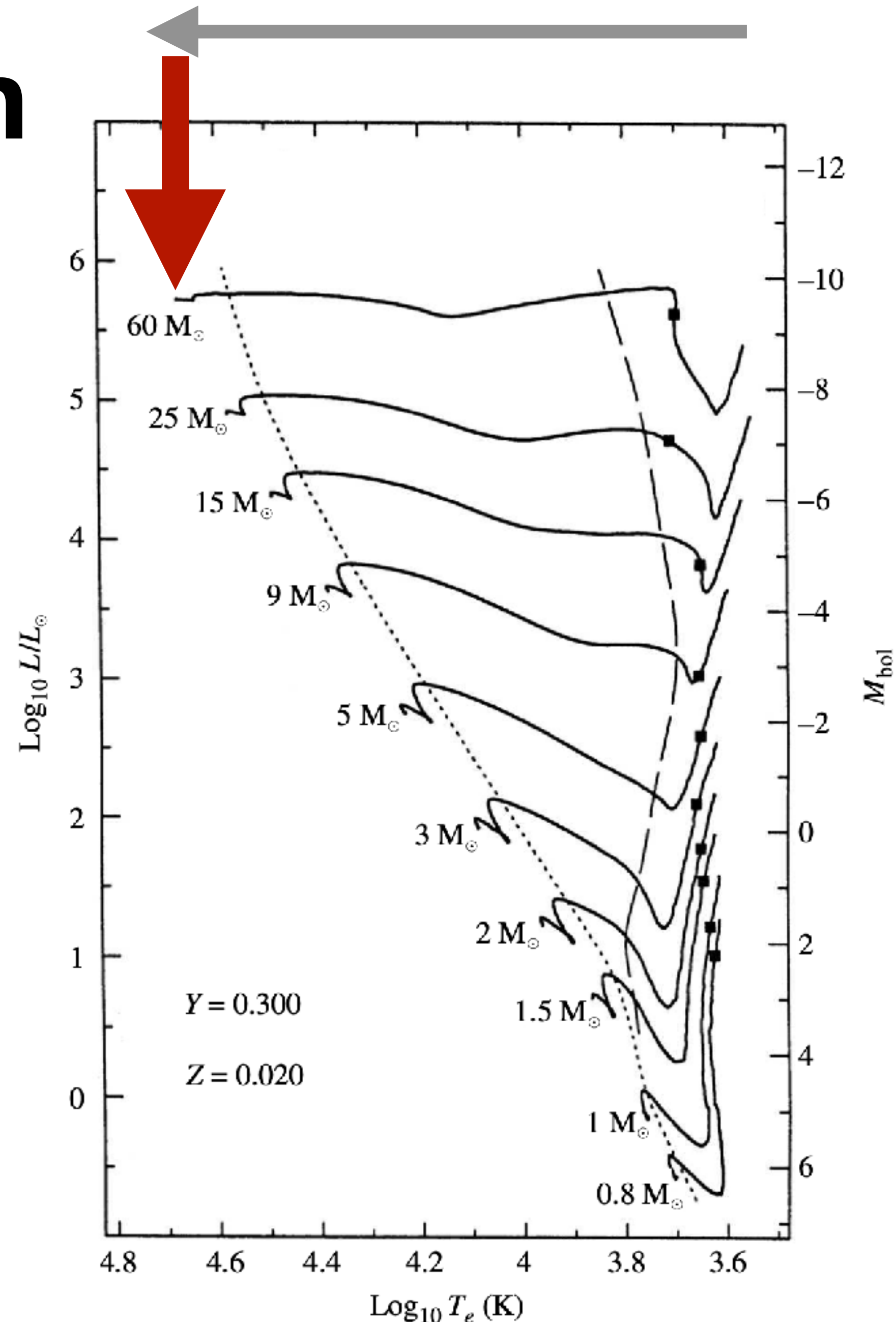


Pre-Main-Sequence evolution

When the ^{12}C is finally exhausted, the core completes its readjustment to nuclear burning, reaching a sufficiently high temperature for the **remainder of the PP I chain** to become important.

At the same time, with the establishment of a stable energy source, the gravitational energy term becomes insignificant and the star **finally settles onto the main sequence**.

It is worth noting that the **time** required for a 1 M_\odot star to reach the main sequence, according to the detailed numerical model just described, is not very different from the simple **estimate of the Kelvin–Helmholtz timescale**.



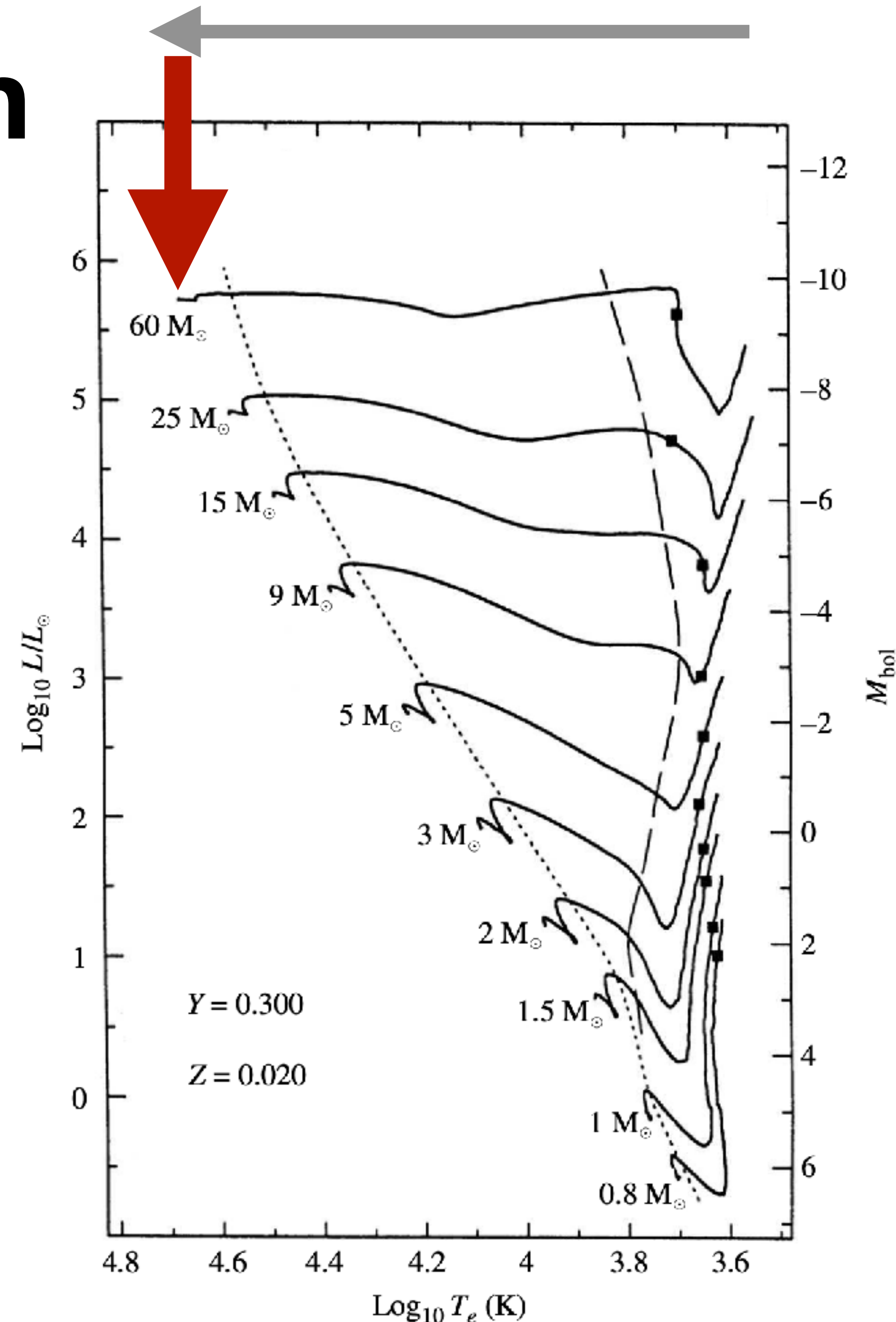
Pre-Main-Sequence evolution

For stars with **masses lower than our Sun's**, the evolution is somewhat different. For stars with masses $M < 0.5 M_{\odot}$ (not shown in the Figure), the **upward branch is missing just before the main sequence**. This happens because the central temperature **never gets hot enough to burn ^{12}C** efficiently.

If the mass of the collapsing protostar is **less than approximately $0.072 M_{\odot}$** , the core never gets hot enough to generate sufficient energy by nuclear reactions to stabilize the star against gravitational collapse. As a result, the **stable hydrogen-burning main sequence is never obtained**. This explains the lower end of the main sequence.

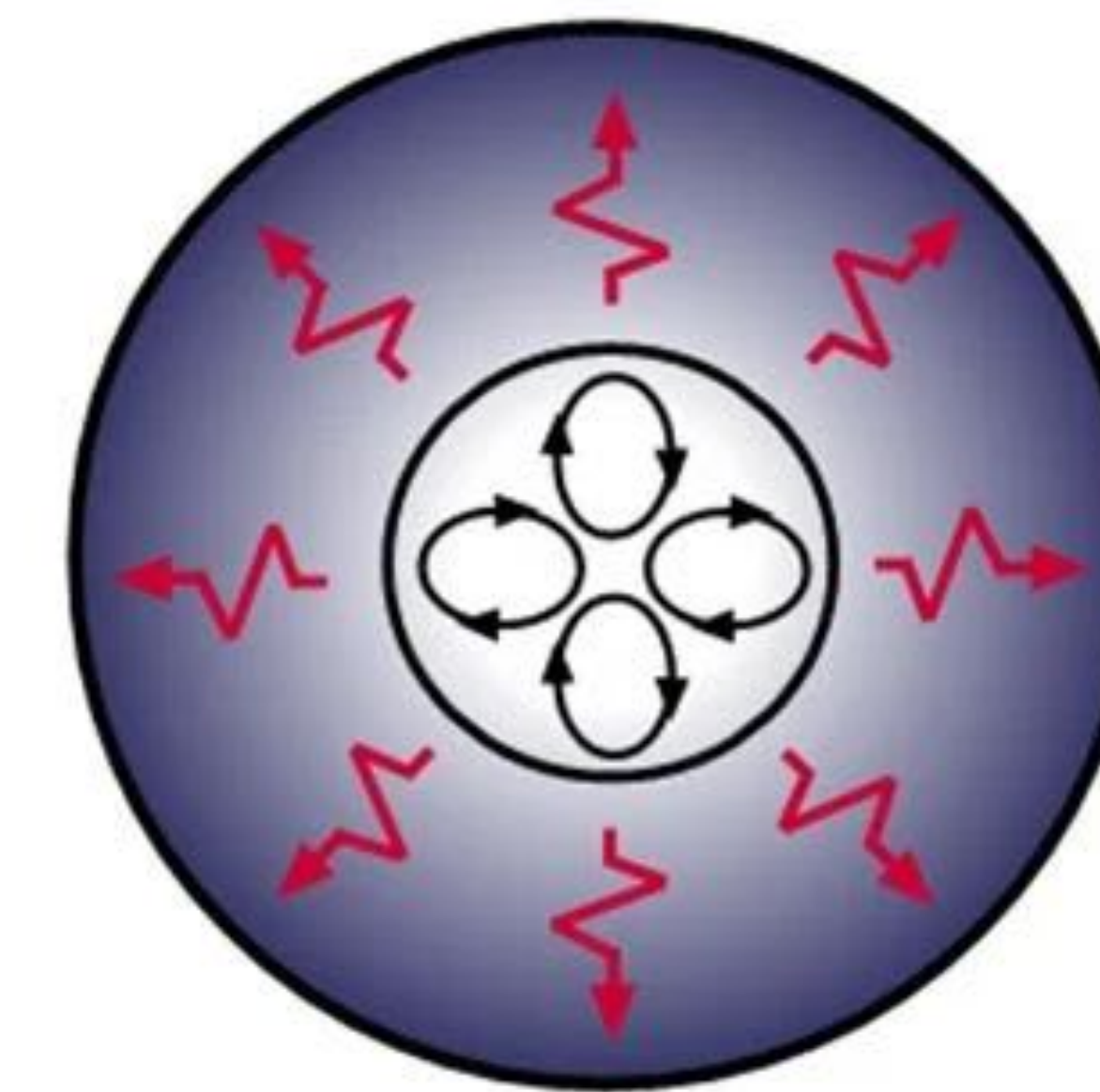
What kind of objects are these?

Another important difference exists between solar-mass stars and stars of lower mass that can reach the main sequence: **Temperatures remain cool enough and the opacity stays sufficiently high in low-mass stars that a radiative core never develops**. Consequently, these stars remain **fully convective** all the way to the main sequence.



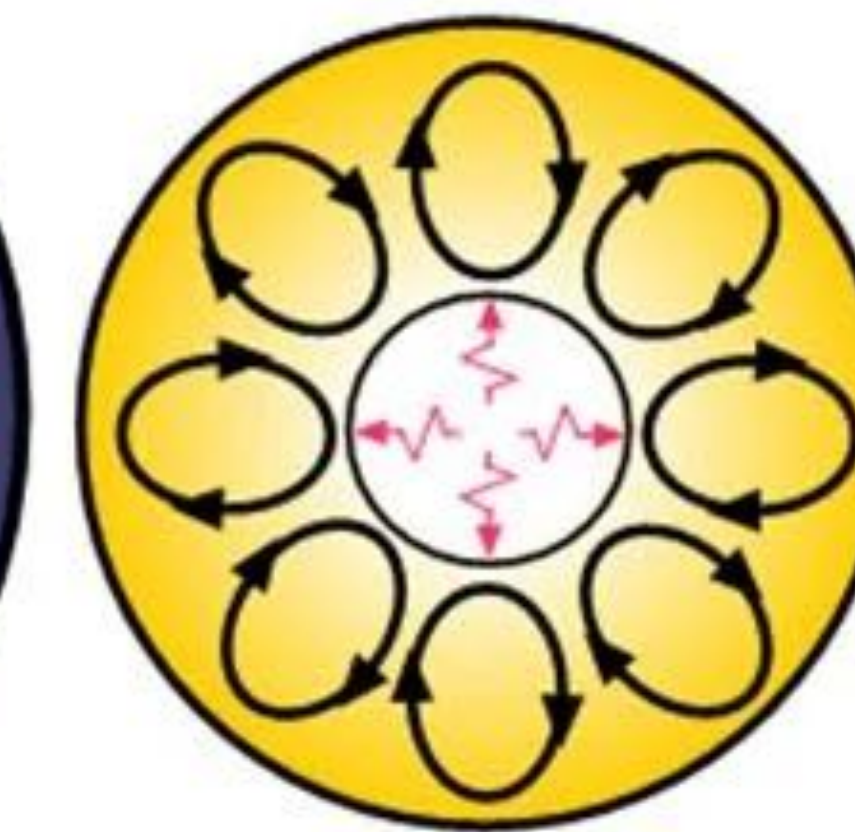
Pre-Main-Sequence evolution

Stellar Structure



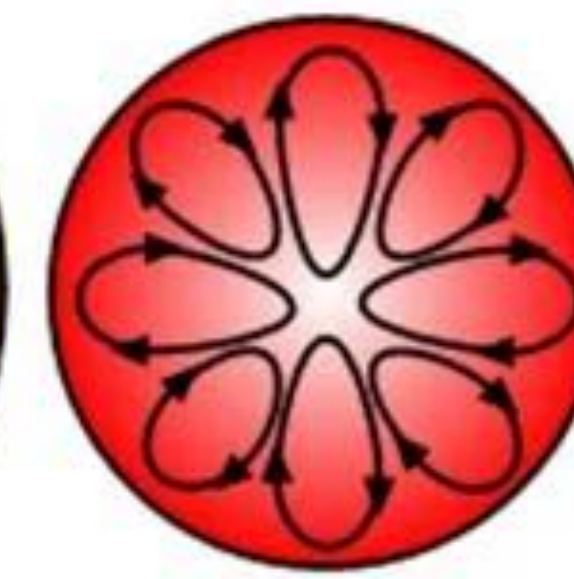
$$M > 1.5$$

Convective Core
Radiative Envelope



$$0.5 < M < 1.5$$

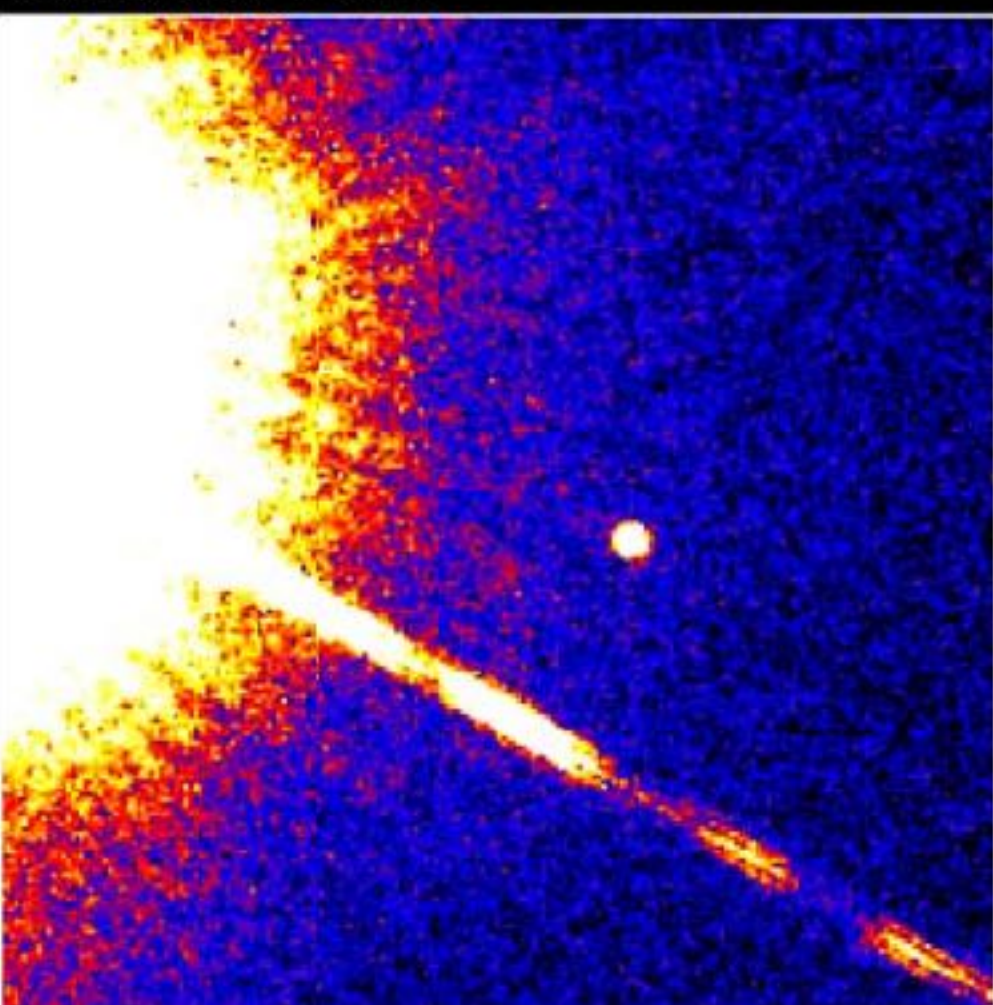
Radiative Core
Convective Envelope



$$M < 0.5$$

Fully Convective

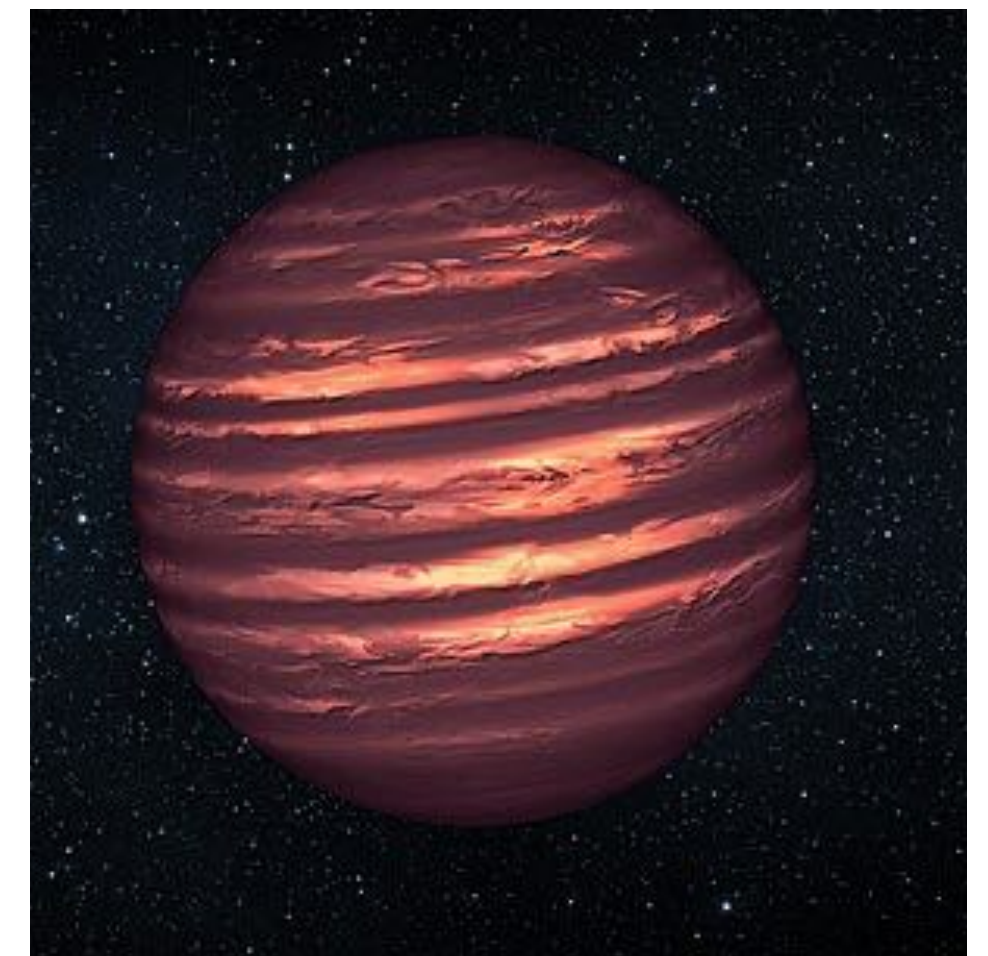
Gliese 229B



Hubble Space Telescope
Wide Field Planetary Camera 2
November 17, 1995

and D. Golimowski (JHU), NASA

Artist representation
If a brown dwarf



Formation of Brown Dwarfs

Below about $0.072 M_{\odot}$, some nuclear burning will still occur, but not at a rate necessary to form a main-sequence star.

- **Above about $0.06 M_{\odot}$** the core temperature of the star is great enough to **burn lithium**,
- and **above a mass of $0.013 M_{\odot}$ deuterium burning** occurs ($0.013 M_{\odot}$ is roughly thirteen times the mass of Jupiter).

This last value is also in agreement with the cessation of fragmentation discussed earlier.

The **objects in the range between $0.013 M_{\odot}$ and $0.072 M_{\odot}$** are known as **brown dwarfs** and have spectral types of L and T.

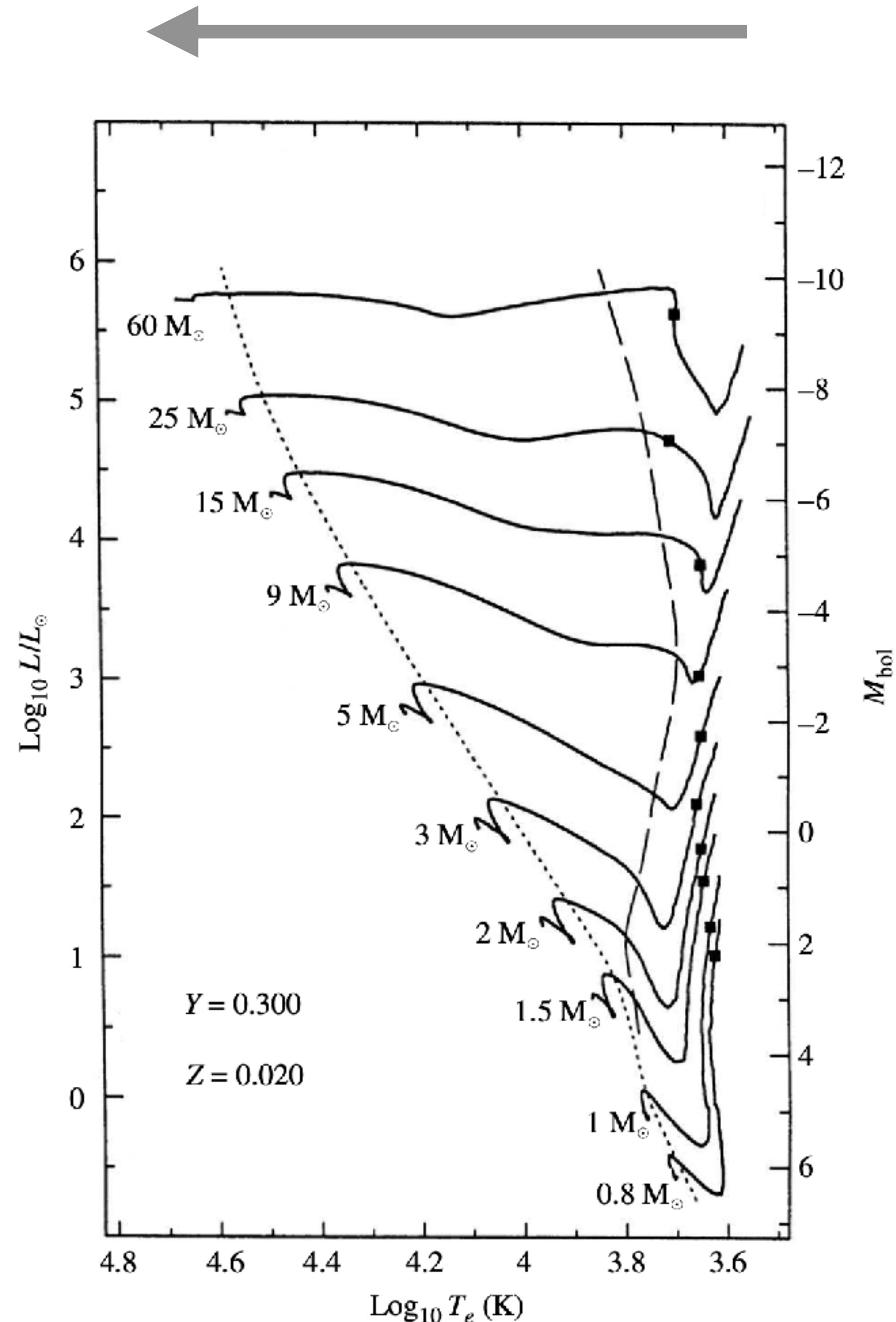
The **first confirmed discovery** of a brown dwarf, **Gliese 229B**, was announced in 1995.

Since that hundreds of brown dwarfs have been detected thanks to near-infrared all-sky surveys, such as the Two Micron All Sky Survey (2MASS) and the Sloan Digital Sky Survey (SDSS). Given their very low luminosities and difficulty of detection, the number of objects found to date suggest that brown dwarfs are prevalent throughout the Milky Way Galaxy.

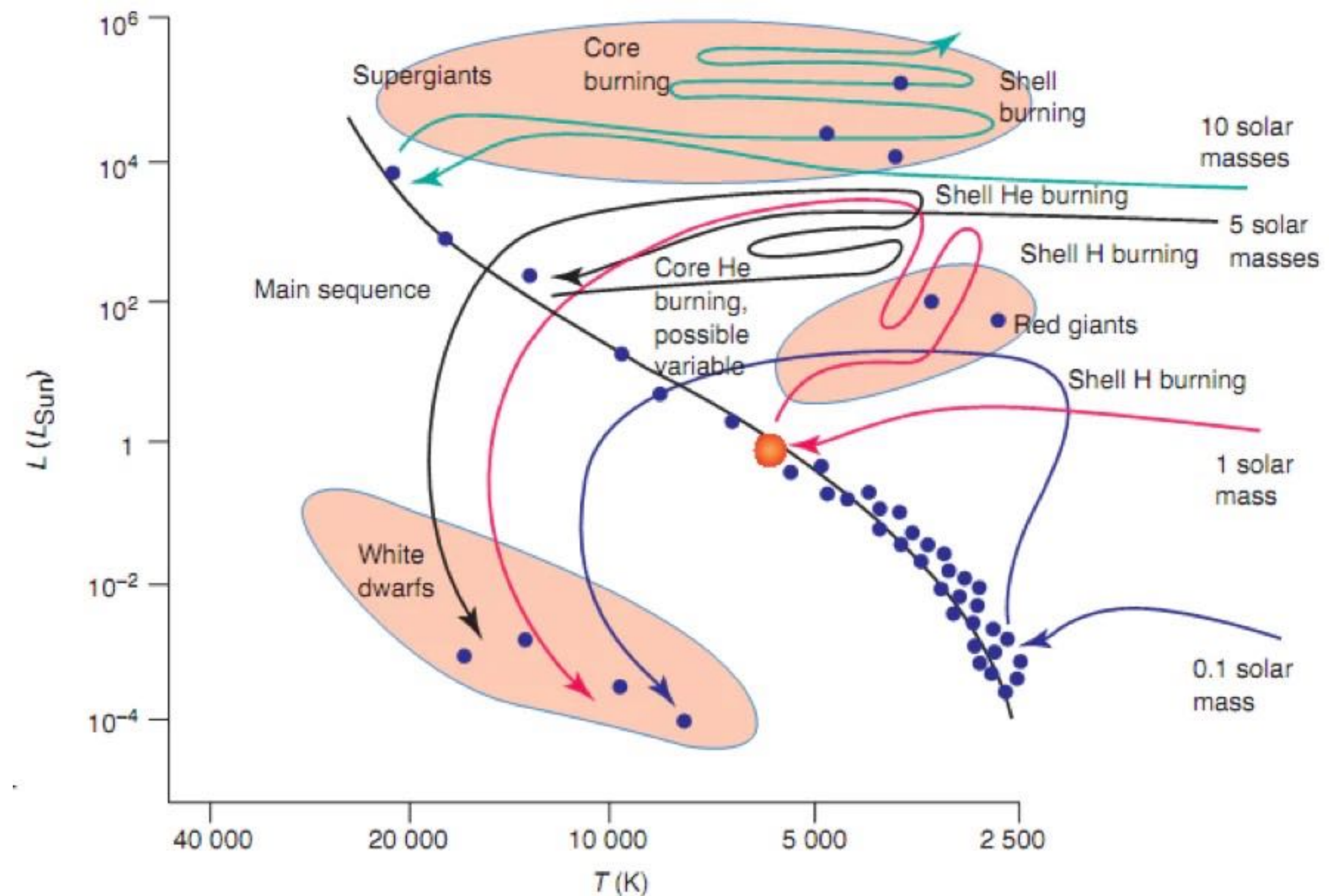
Massive star formation

For massive stars, the central temperature quickly becomes high enough to burn ^{12}C as well as convert ^1H into ^3He .

This means that **these stars leave the Hayashi track at higher luminosities and evolve nearly horizontally across the H–R diagram**. Because of the much larger central temperatures, **the full CNO cycle becomes the dominant mechanism for hydrogen burning** in these main-sequence stars. Since the CNO cycle is so strongly temperature- dependent, the **core remains convective** even after the main sequence is reached.



Evolution on the HR diagram



Limitation of models

The general pre-main-sequence evolutionary track calculations described above contain **numerous approximations**.

It is likely that **rotation** plays an important role, along with **turbulence and magnetic fields**. It is also likely that the initial environments contain **inhomogeneities** in cloud densities, **strong stellar winds**, and **ionizing radiation** from nearby, massive stars.

These classical models **also assume initial structures that are very large**, with radii that are effectively infinitely greater than their final values. Given that dense cores have dimensions on the order of 0.1 pc, the **initial radii of clouds undergoing protostellar collapse must be much smaller** than traditionally assumed. In addition, the assumption of pressure-free protostellar collapse may also be a poor one; more realistic calculations probably require an initial contraction that is quasi-static (after all, the dark cores are roughly in hydrostatic equilibrium).

To complicate matters further, the more **massive stars** also **interact with infalling material in such a way that a feedback loop may develop**, limiting the amount of mass that they can accrete via the classical process discussed to this point; remember the Eddington limit for accretion.

Improvements of models

Theoretical evolutionary sequences beginning with **smaller initial radii lead to a birth line** where **protostars first become visible**. This birth line places an upper limit on the observed luminosities of protostars.

In addition, some observations suggest that **stars with masses greater than about $10 M_{\odot}$ or so may not form at all by the classical pre-main-sequence process** described above. This apparent effect could be due to limiting **feedback mechanisms**, such as **the high luminosity of ionizing radiation** associated with high effective temperatures.

Instead of the collapse of single protostellar clouds, **the more massive stars may form by mergers of smaller stars in dense protostellar environments**. On the other hand, some researchers have argued that the need for mergers can be avoided because rotation implies that most of the infalling mass collapses to an **accretion disk** that forms around the star. The **accretion disk then feeds the growing massive star, minimizing the impact of high amounts of ionizing radiation** on the infalling gas and dust.

High mass star formation is still under active research.

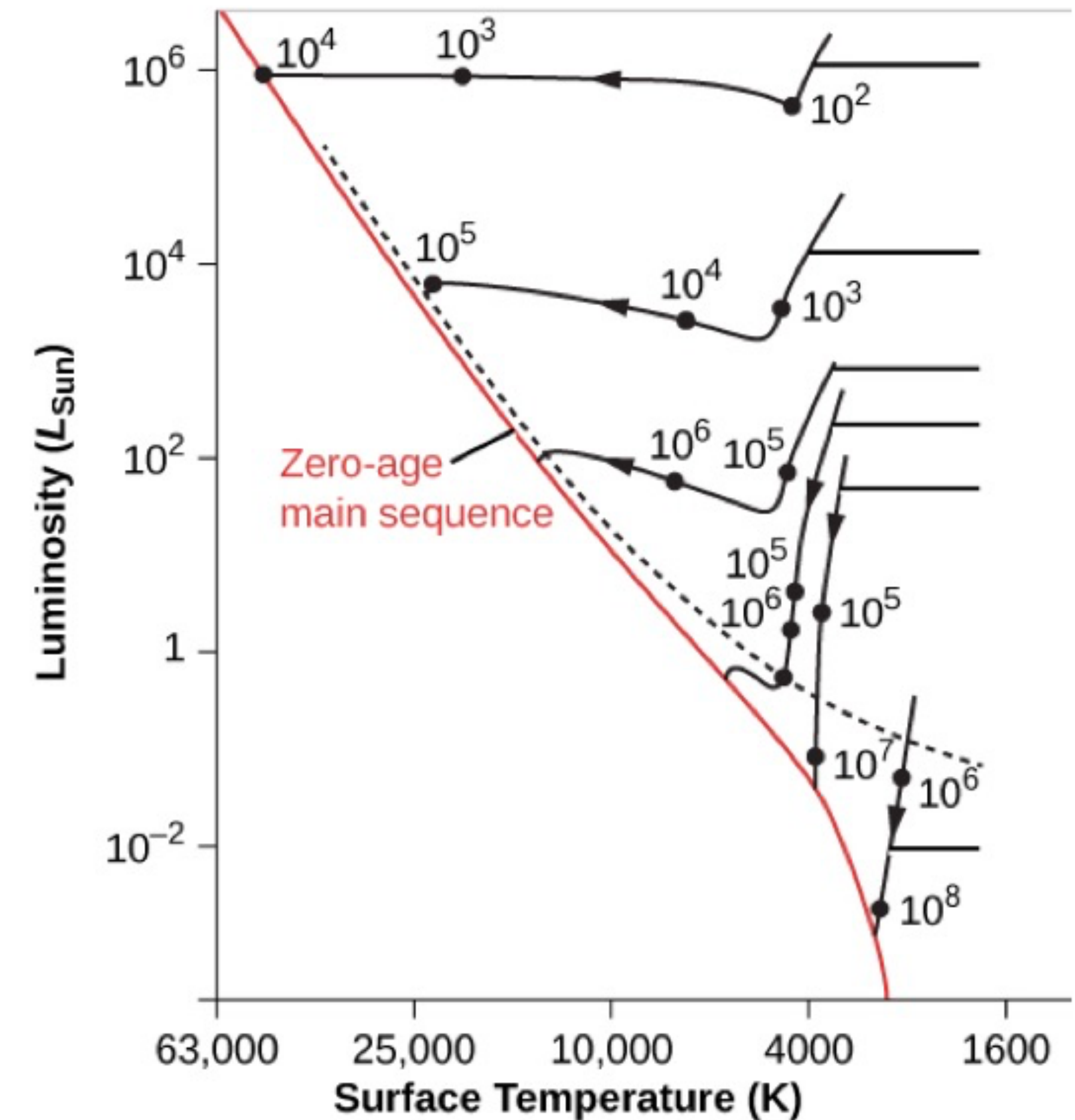
The Zero-Age main sequence (ZAMS)

The diagonal line in the H–R diagram where stars of various masses first reach the main sequence and begin equilibrium hydrogen burning is known as the **zero-age main sequence** (ZAMS).

Based on the classical model **the time required for stars to collapse onto the ZAMS is inversely related to mass**; a $0.8 M_{\odot}$ star takes over 68 Myr to reach the ZAMS, whereas a $60 M_{\odot}$ star makes it to the ZAMS in only 28,000 years!

This inverse relationship may signal a problem with classical pre-main-sequence evolutionary models. The reason is that **if the most massive stars do indeed form first in a cluster of stars, the intense radiation that they produce would likely disperse the cloud before the low-mass could form**.

Star formation is still active research.



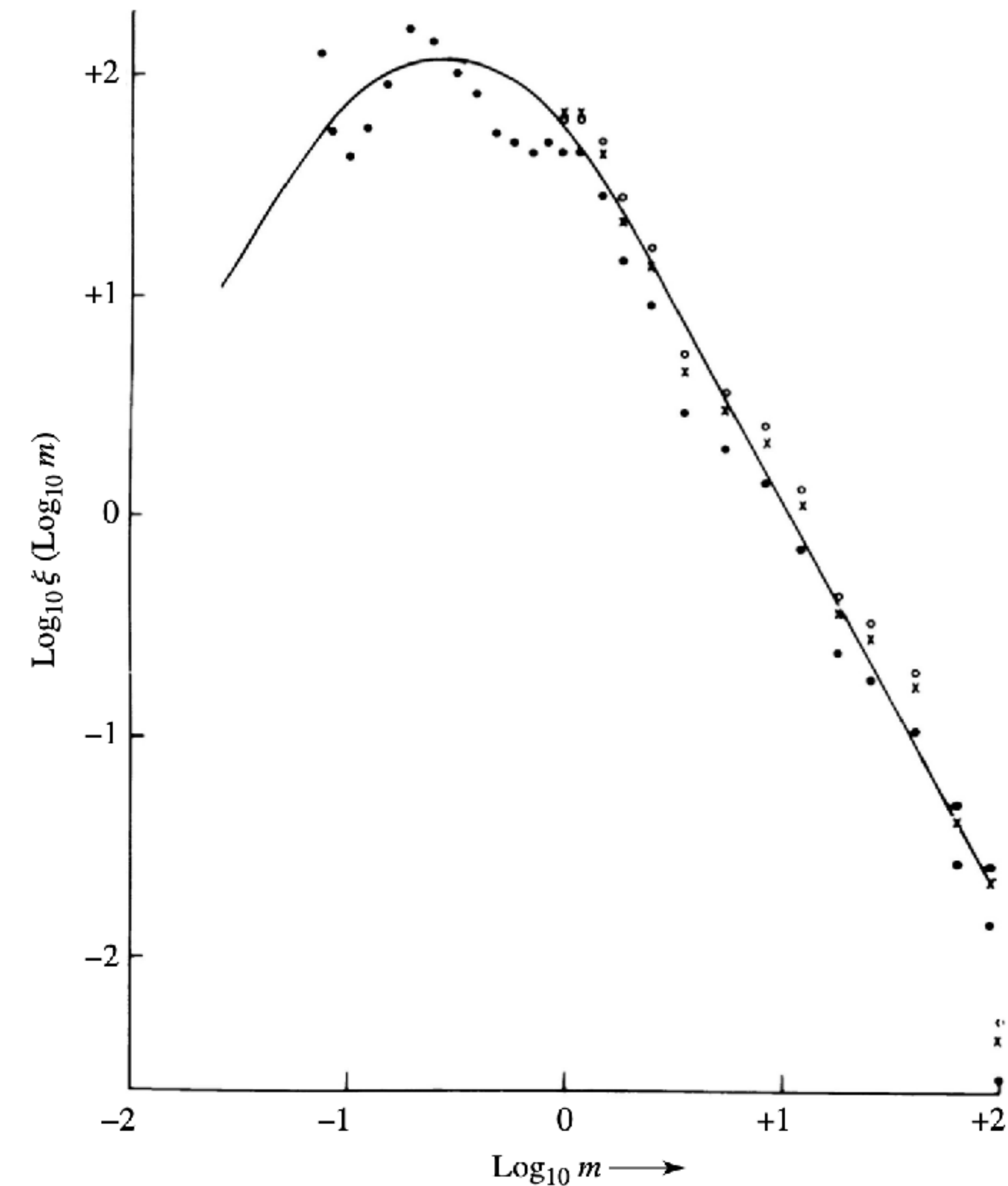
The Initial Mass Function (IMF)

From observational studies it is apparent that more low-mass than high-mass stars form when an interstellar cloud fragments.

This implies that the number of stars that form per mass interval per unit volume (or per unit area in the Milky Way's disk) (ξ) is strongly mass-dependent. This functional dependence is known as the **initial mass function (IMF)**.

One theoretical estimate of the IMF is shown in the Figure.

However, a particular IMF **depends on** a variety of factors, including **the local environment** in which a cluster of stars forms from a given cloud complex in the ISM.

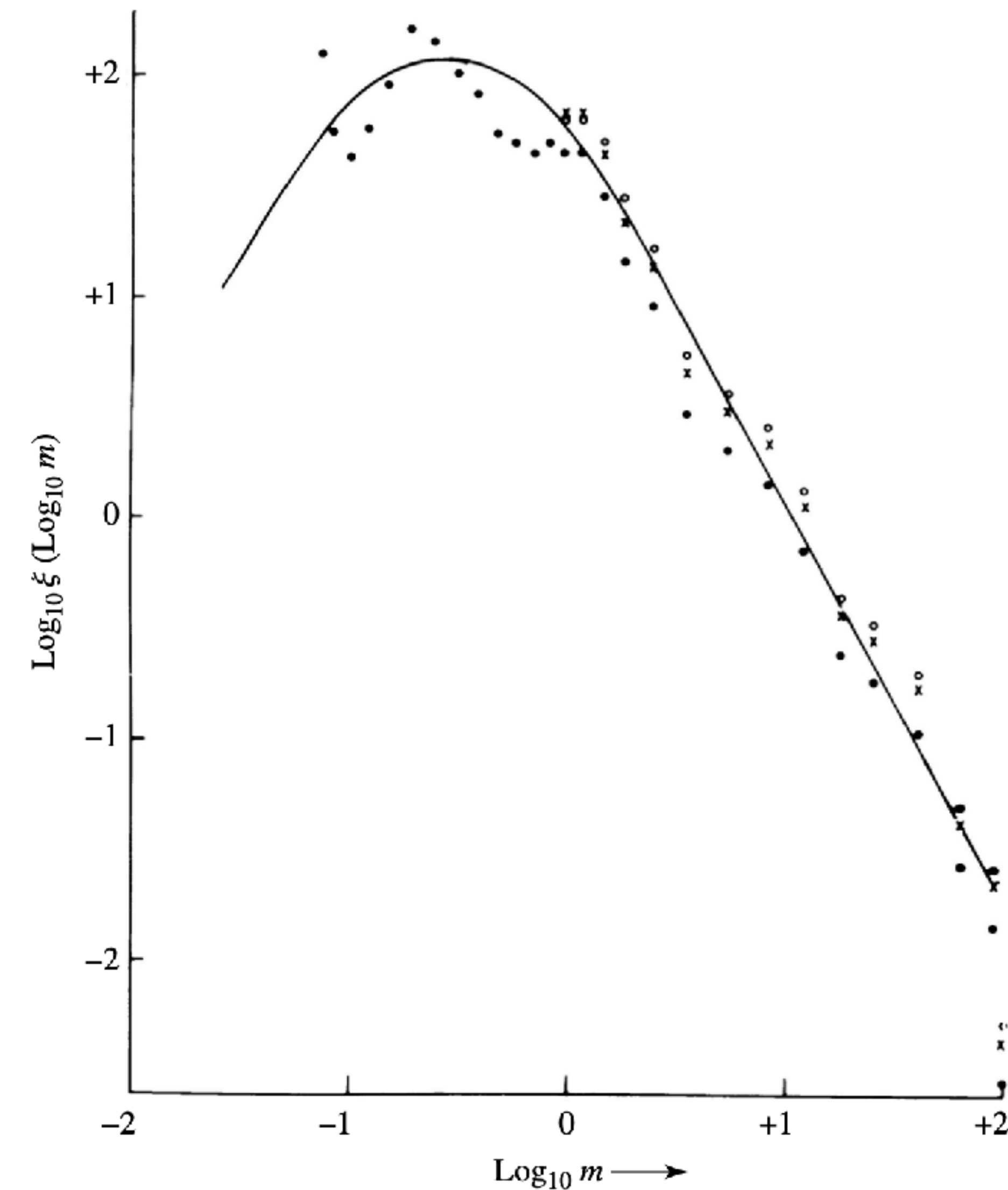


The Initial Mass Function (IMF)

As a consequence of the process of fragmentation, most stars form with relatively low mass.

Given the disparity in the **numbers of stars formed** in different mass ranges, combined with the very different **rates of evolution**, it is not surprising that **massive stars are extremely rare, while low-mass stars are found in abundance**.

Observations also suggest that although the IMF is quite uncertain **below about $0.1 M_{\odot}$** , rather than falling off sharply as indicated in the Figure, **the curve may be fairly flat**, resulting in large numbers of low-mass stars and brown dwarfs.



The effects of massive stars

As a **massive star forms**,

- the protostar will initially appear as an **infrared source** embedded inside the molecular cloud.
- With the rising temperature, first the **dust will vaporize**,
- then the **molecules will dissociate**,
- and finally, as the star reaches the main sequence, the **gas immediately surrounding it will ionize**, resulting in the creation of an H II region inside of an existing H I region.
- Now, **because of the star's high luminosity, radiation pressure** will begin to drive significant amounts of mass loss, **which then tends to disperse the remainder of the cloud**.

If several O and B stars form at the same time, it may be that much of the mass that has not yet become gravitationally bound to more slowly forming low-mass protostars will be driven away, **halting any further star formation**.

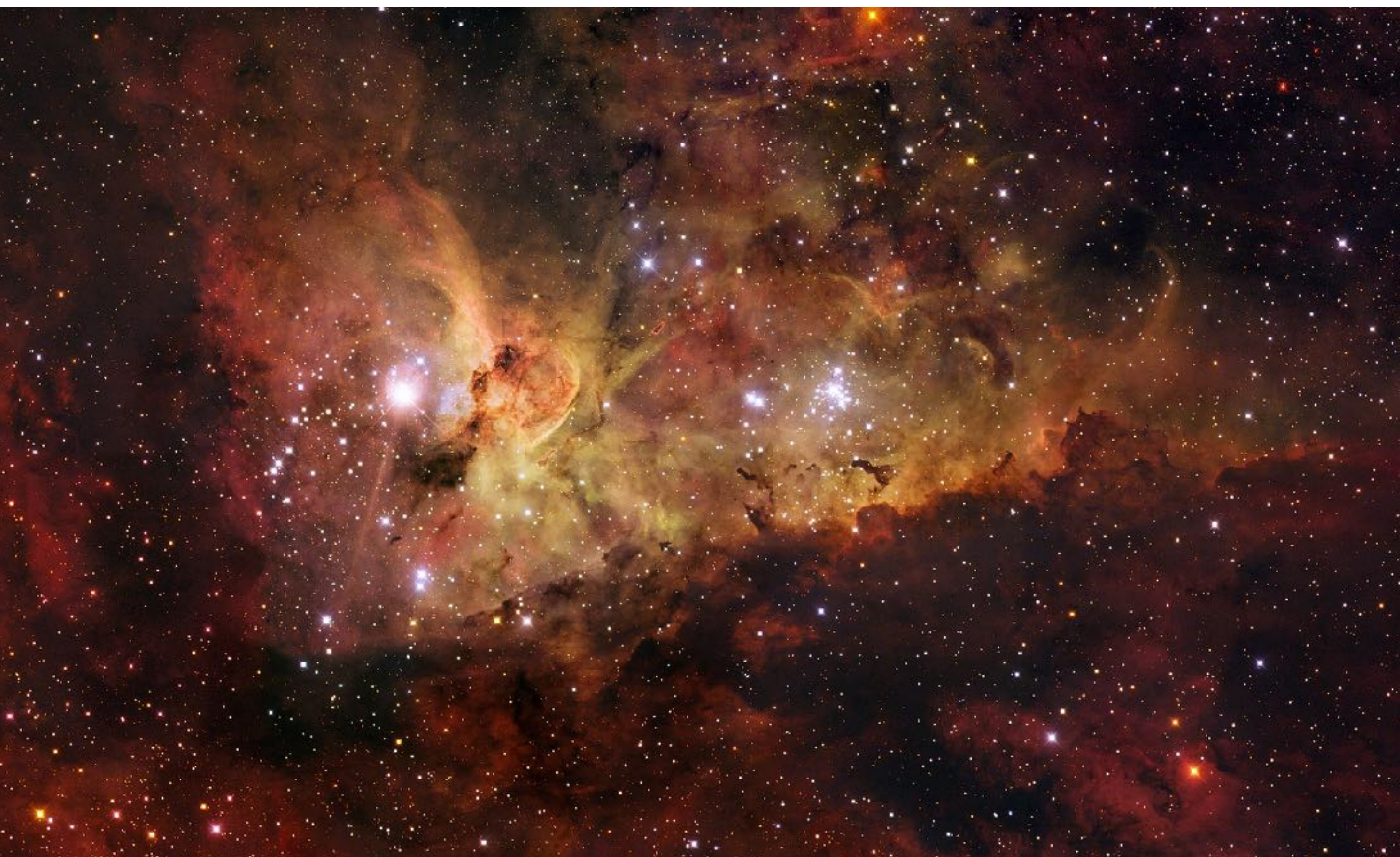
If the **cloud was originally marginally bound** (near the limit of criticality), the loss of mass will diminish the potential energy term in the virial theorem, with the result that the **newly formed cluster of stars and protostars will become unbound** (i.e., the stars will tend to **drift apart**).

The effects of massive stars

The Carina Nebula is a large bright nebula that surrounds several clusters of stars. It contains two of the most massive and luminous stars in our Milky Way galaxy, Eta Carinae and HD 93129A. Located 7500 light years away, the nebula itself spans some 260 light years across, about 7 times the size of the Orion Nebula.

Being brighter than one million Suns, Eta Carinae (the brightest star in this image) is the most luminous star known in the Galaxy, and has most likely a mass over 100 times that of the Sun.

Radiation from the bright stars is shredding the dust clouds in the lower part of the images.

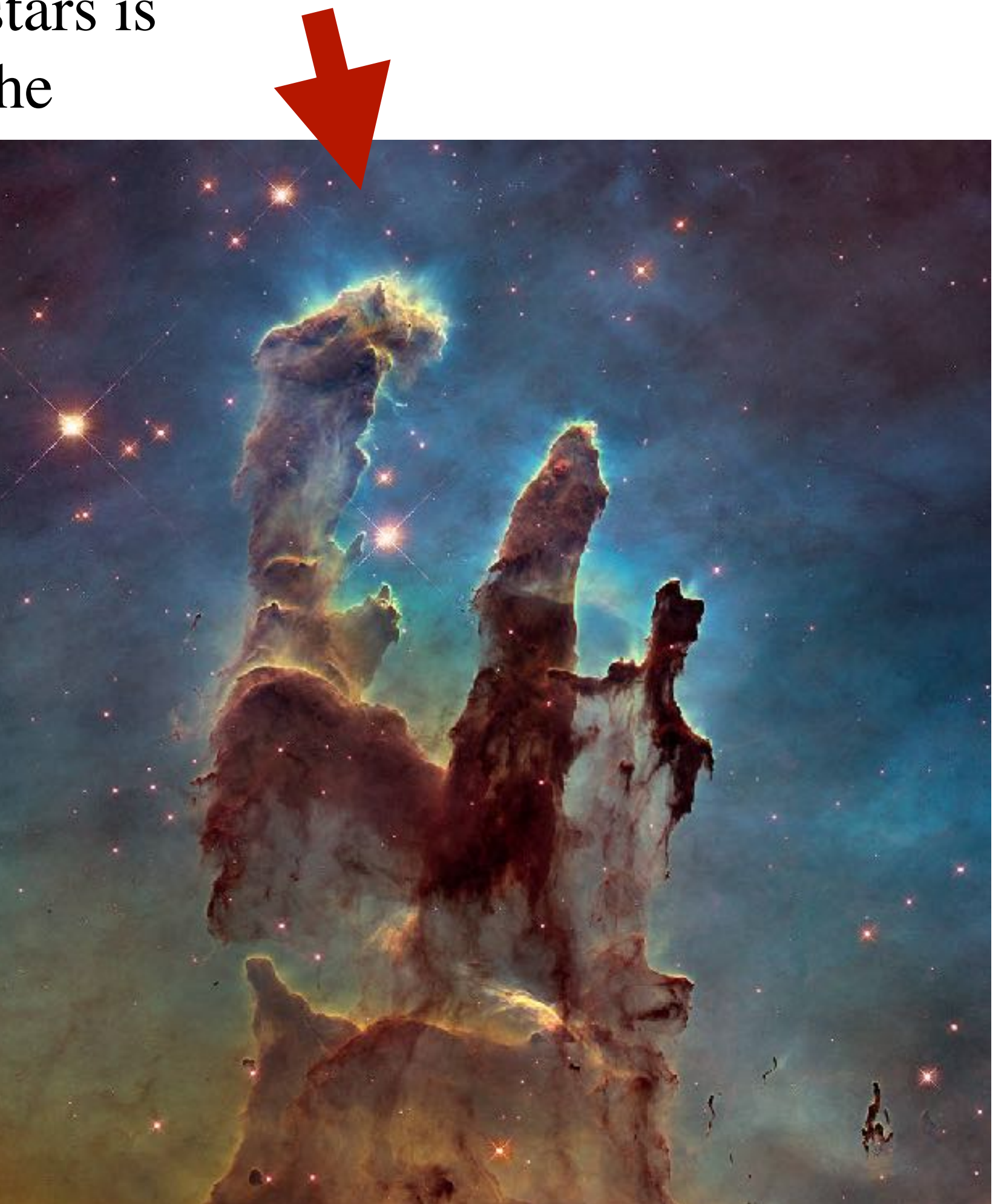


The effects of massive stars

James Webb Telescope

Another famous example of the effects of ionizing radiation of nearby massive stars is the production of the pillars in M16, the Eagle Nebula.

The left most pillar is more than 1 pc long from base to top. Ionizing radiation from massive newborn stars off the top edge of the image are causing the gas in the cloud to photoevaporate.



Hubble Space Telescope



Herbig Haro Objects

Mass loss during pre-main-sequence evolution can also occur from **jets** of gas that are ejected in narrow beams in opposite directions.

Herbig–Haro objects, are apparently associated with the **jets produced by young protostars**, such as T Tauri stars (low mass young stars). As the **jets expand supersonically into the interstellar medium, collisions excite the gas**, resulting in bright objects with emission-line spectra.

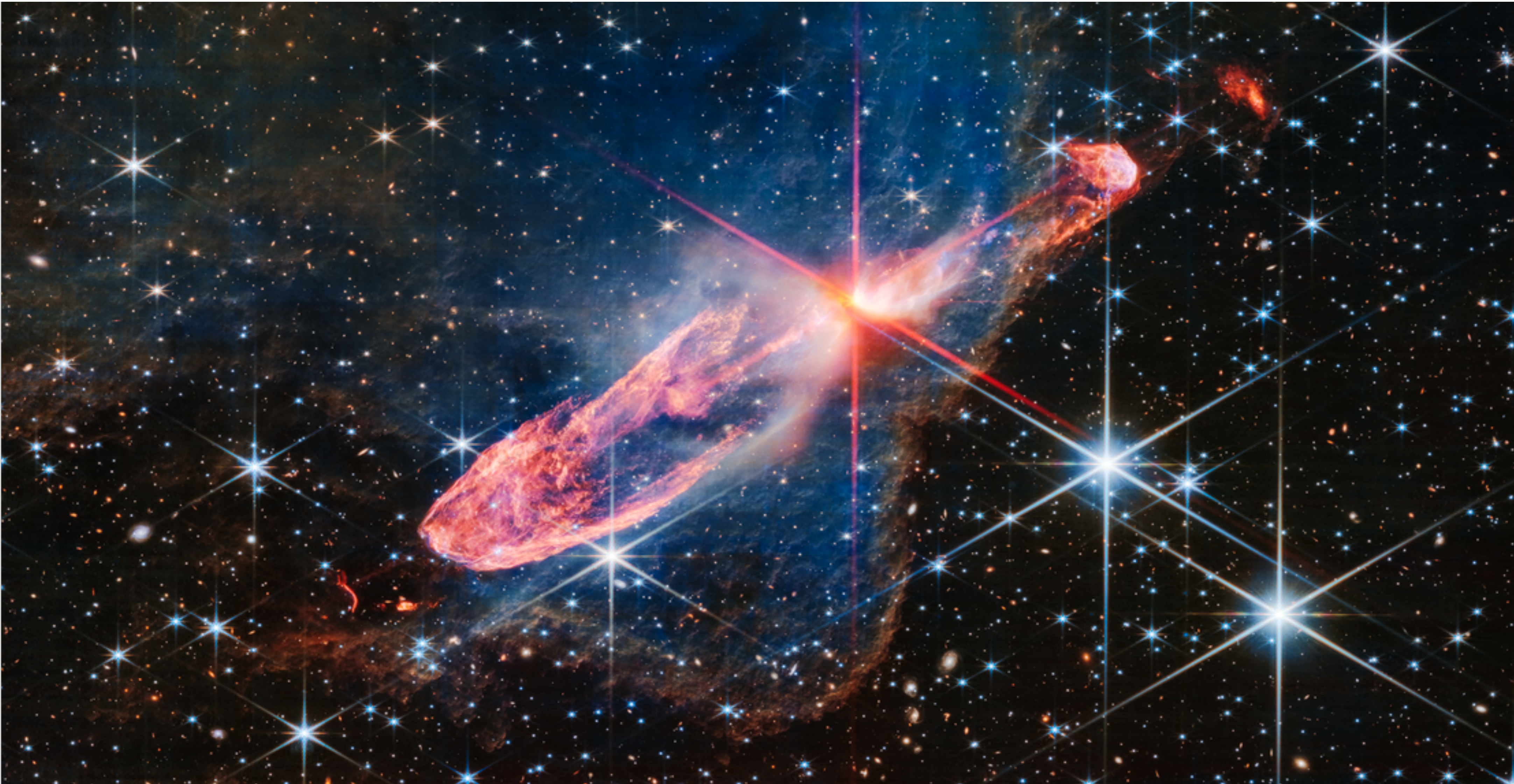
The Figure shows a Hubble Space Telescope image of the Herbig–Haro objects HH 1 and HH 2, which were created by material ejected at speeds of several hundred kilometers per second from a star shrouded in a cocoon of dust.



Herbig Haro Objects

The jets associated with another Herbig–Haro object, HH 47, are shown in Figure

James Webb Telescope



Herbig Haro Objects

Herbig–Haro (HH) objects are bright patches of nebulosity associated with newborn stars.

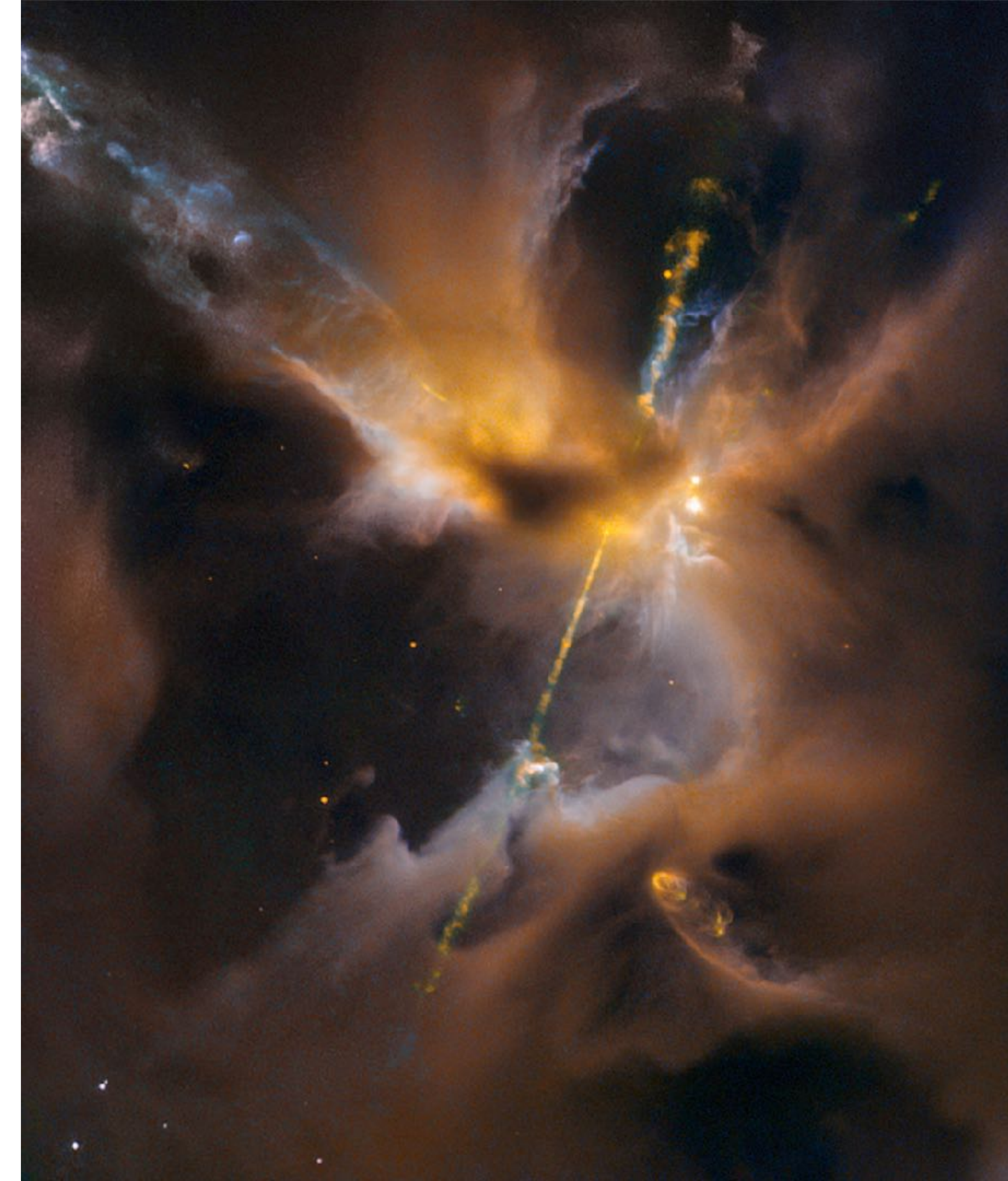
They are formed when narrow jets of partially ionised gas ejected by stars collide with nearby clouds of gas and dust at several hundred kilometres per second.

Herbig–Haro objects are **commonly found in star-forming regions**, and **several are often seen around a single star, aligned with its rotational axis**.

Most of them lie within about **one parsec (3.26 light-years) of the source**, although some have been observed several parsecs away. HH objects are transient phenomena that **last around a few tens of thousands of years**.

They **can change visibly over timescales of a few years** as they move rapidly away from their parent star into the gas clouds of interstellar space (the interstellar medium or ISM).

HH 24, image by Hubble Space Telescope

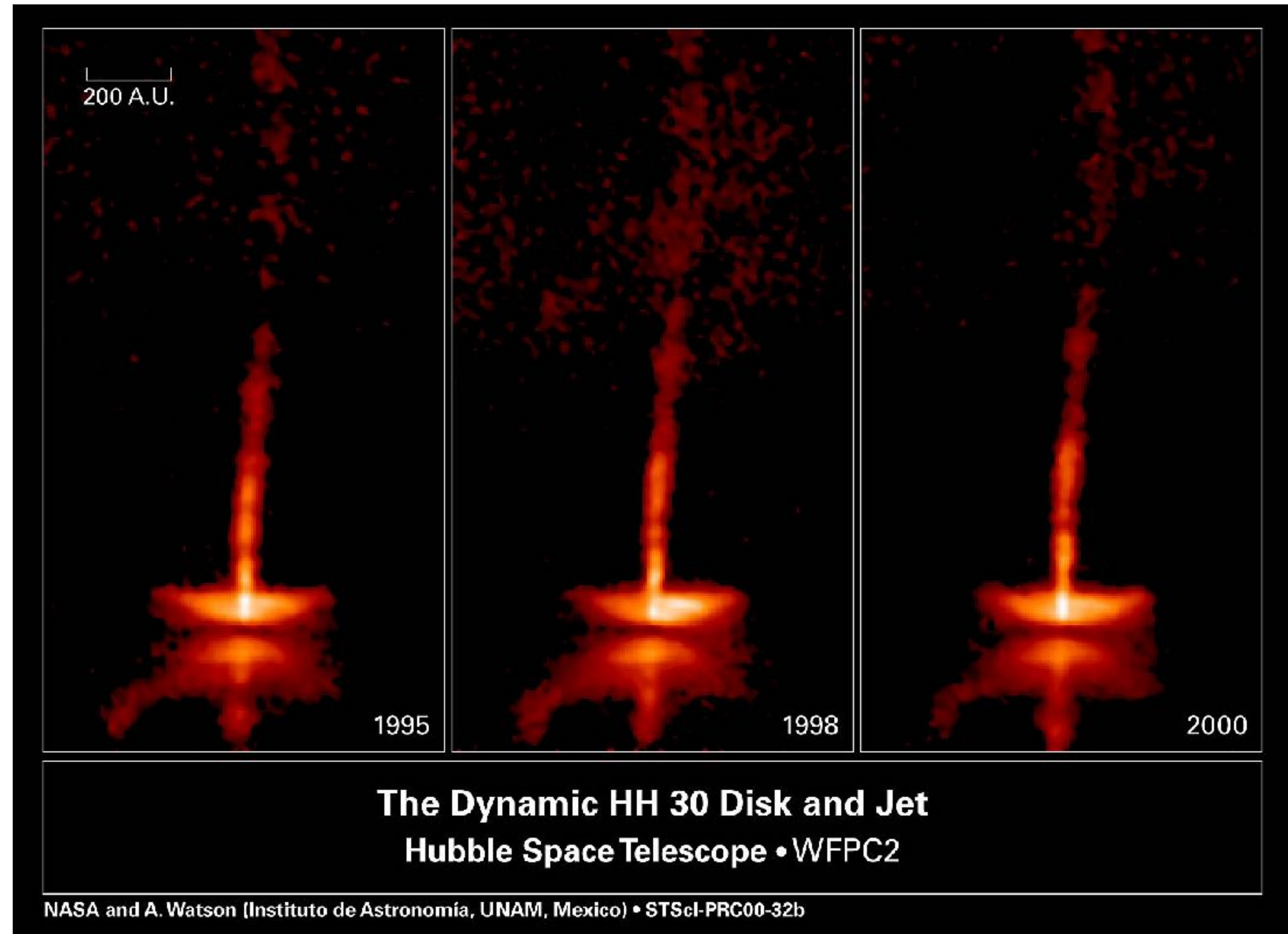


Herbig Haro Objects

Continuous emission is also observed in some protostellar objects and is due to the **reflection of light from the parent star**.

A **circumstellar accretion disk** is apparent around HH 30.

The surfaces of the disk are illuminated by the central star, which is again hidden from view behind the dust in the disk. Also apparent are jets originating from deep within the accretion disk, possibly from the central star itself.



Herbig Haro Objects

These **accretion disks** seem to be responsible for many of the characteristics associated with the protostellar objects,

- including emission lines,
- mass loss,
- jets,
- and perhaps even some of the luminosity variations.

The details concerning the physical processes involved are not fully understood.

An early model of the production of Herbig–Haro objects like HH 1 and HH 2 is shown in the Figure

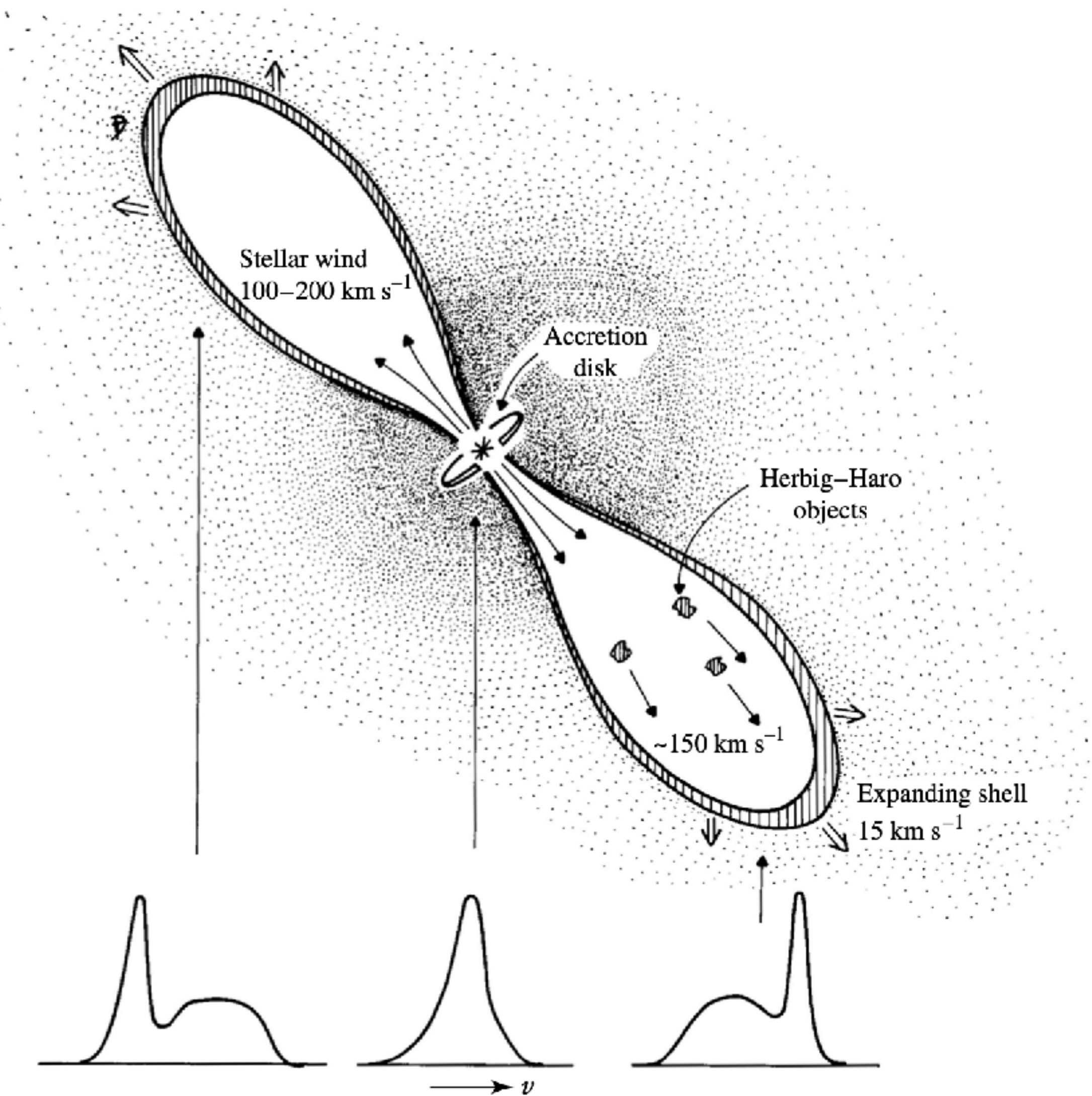
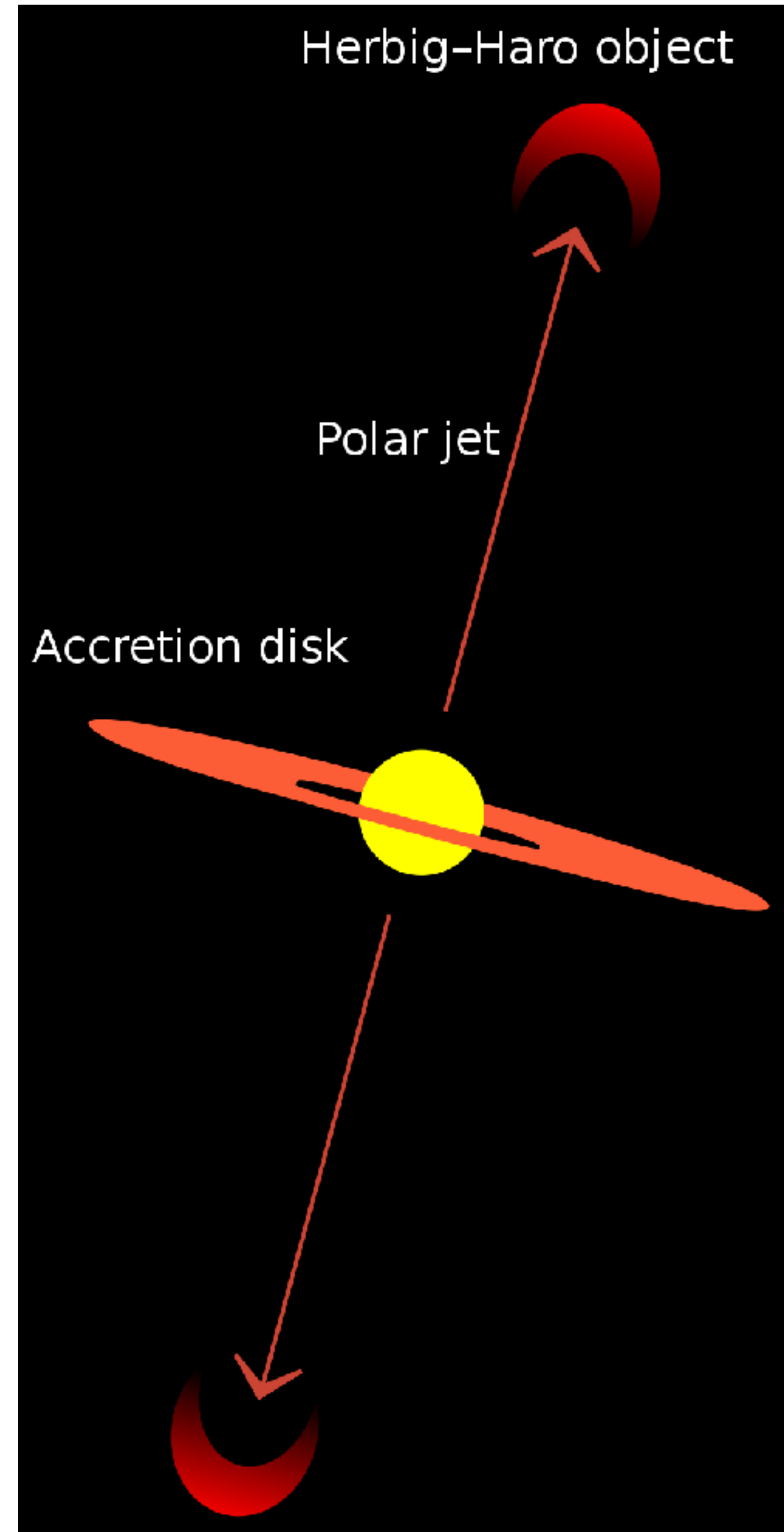
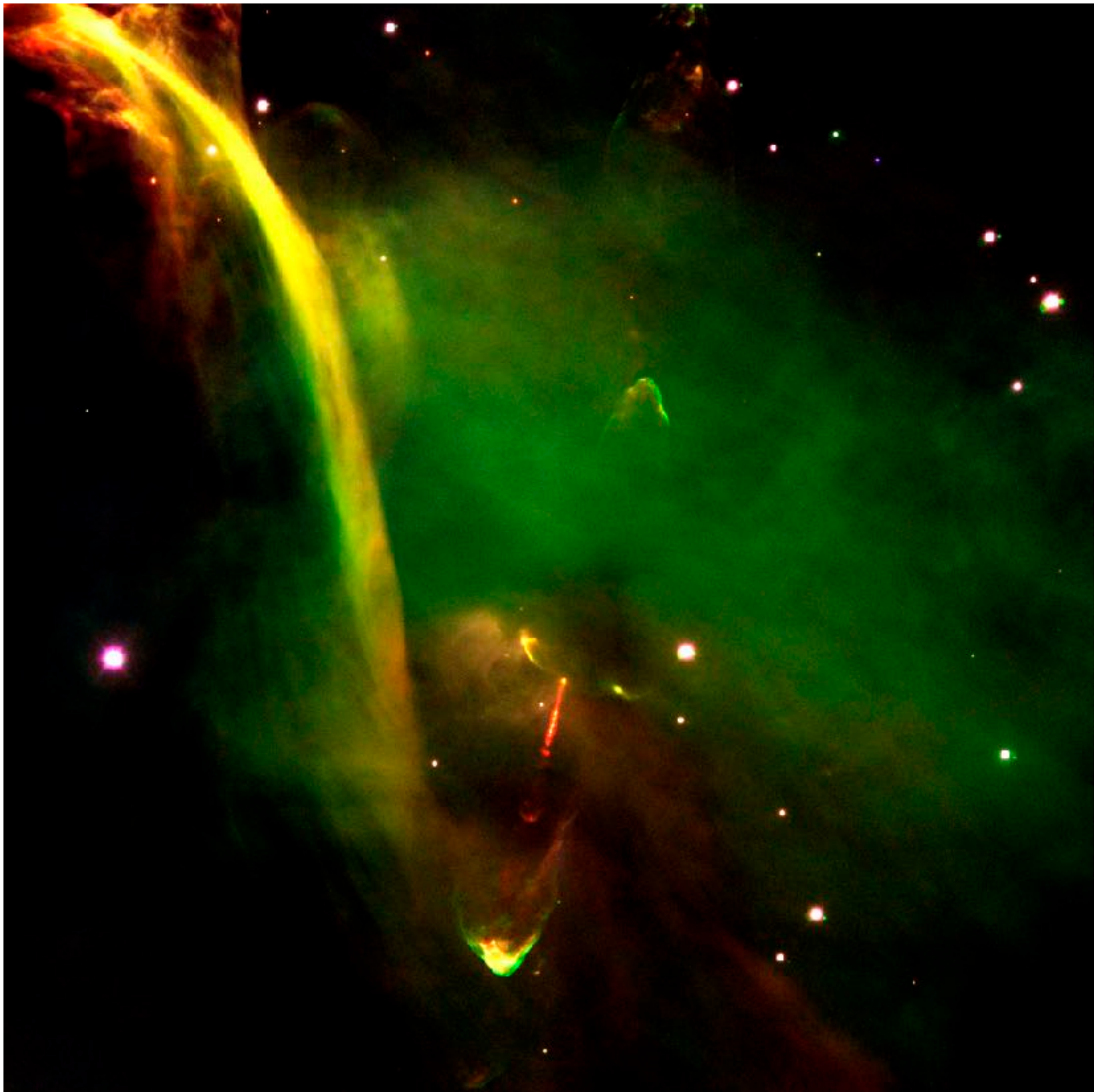


FIGURE 20 An early model of a T Tauri star with an accretion disk. The disk powers and collimates jets that expand into the interstellar medium, producing Herbig–Haro objects. (Figure adapted from Snell, Loren, and Plambeck, *Ap. J. Lett.*, 239, L17, 1980.)

Herbig Haro Objects

Herbig-Haro 34



Herbig-Haro object

Polar jet

Accretion disk

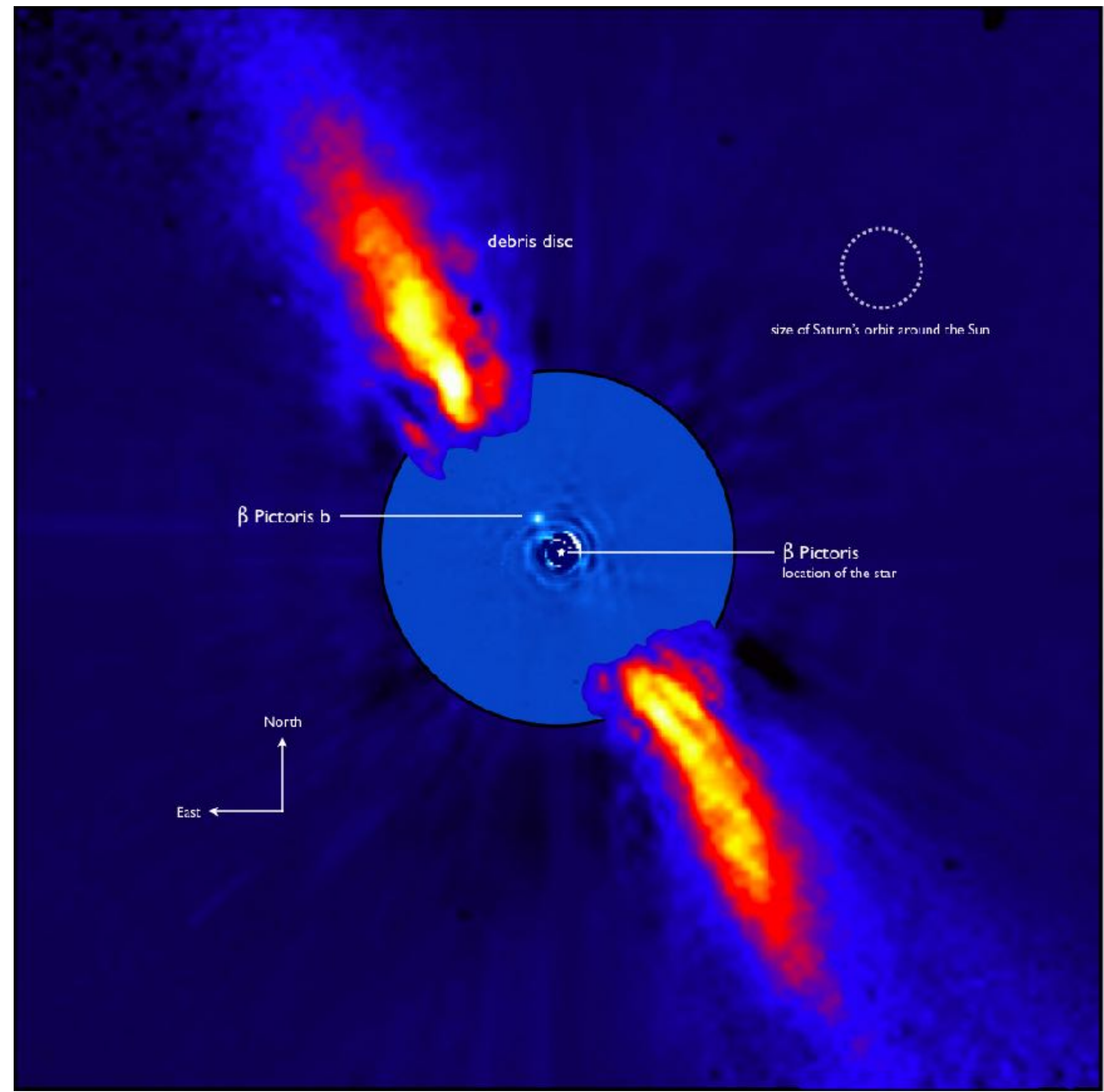
Young stars with circumstellar disks

Observations have revealed that other young stars also possess circumstellar disks of material orbiting them. Two well-known examples are **Vega** and **β Pictoris**.

This composite image represents the close environment of Beta Pictoris as seen in **near infrared light**. This very faint environment is revealed after a very careful subtraction of the much brighter stellar halo.

The outer part of the image shows the reflected light on the dust disc, as observed in 1996; the inner part is the innermost part of the system, as seen at 3.6 microns.

Beta Pictoris b (planet) is more than 1000 times fainter than Beta Pictoris, aligned with the disc, at a projected distance of 8 times the Earth-Sun distance.



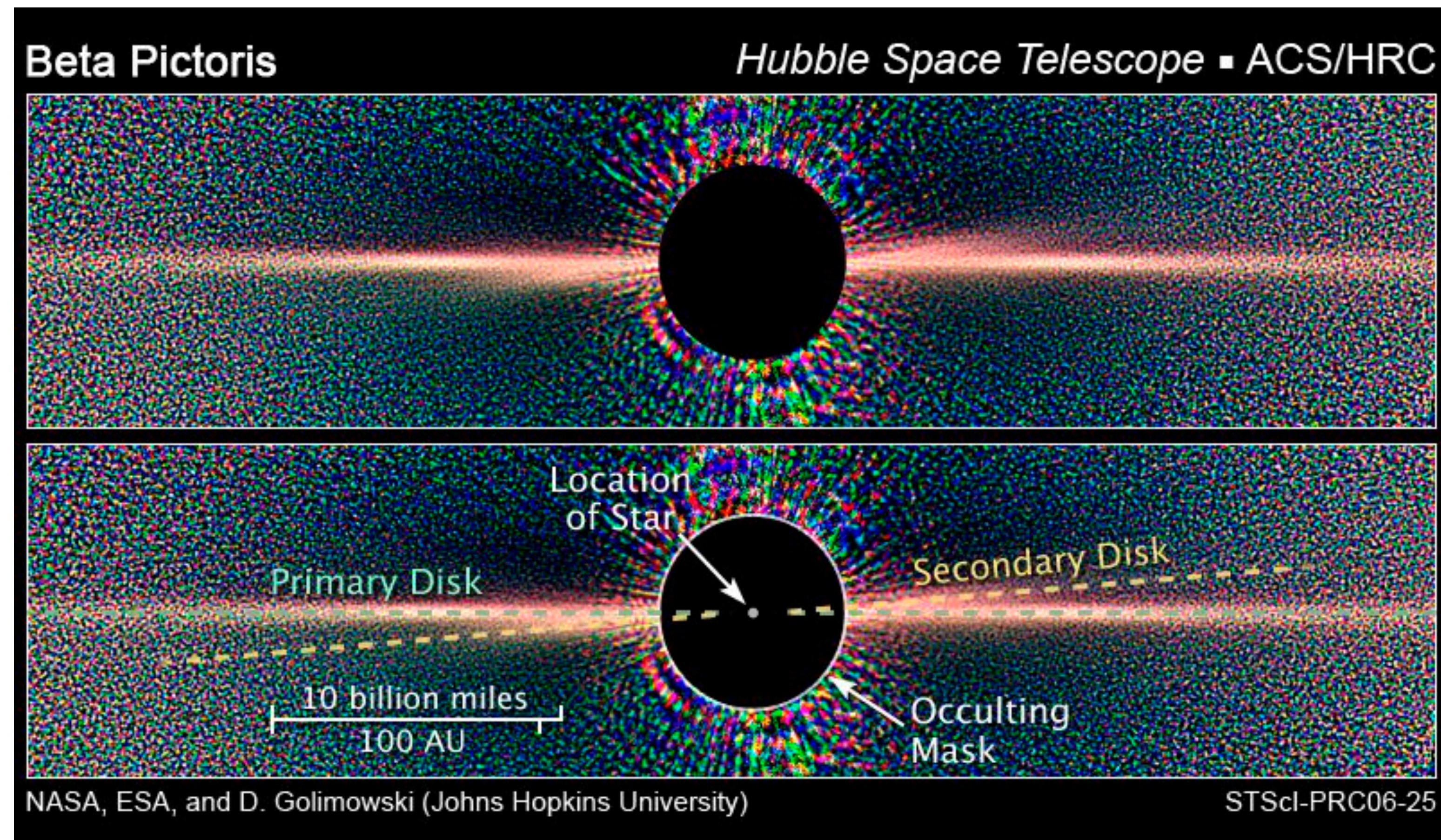
Young stars with circumstellar disks

Two planets, Beta Pictoris b, and Beta Pictoris c, through the use of **direct imagery**.

It appears that **clumps of material are falling from the disk into the star at the rate of two or three per week**. Larger objects may be forming in the disk as well, possibly **protoplanets**.

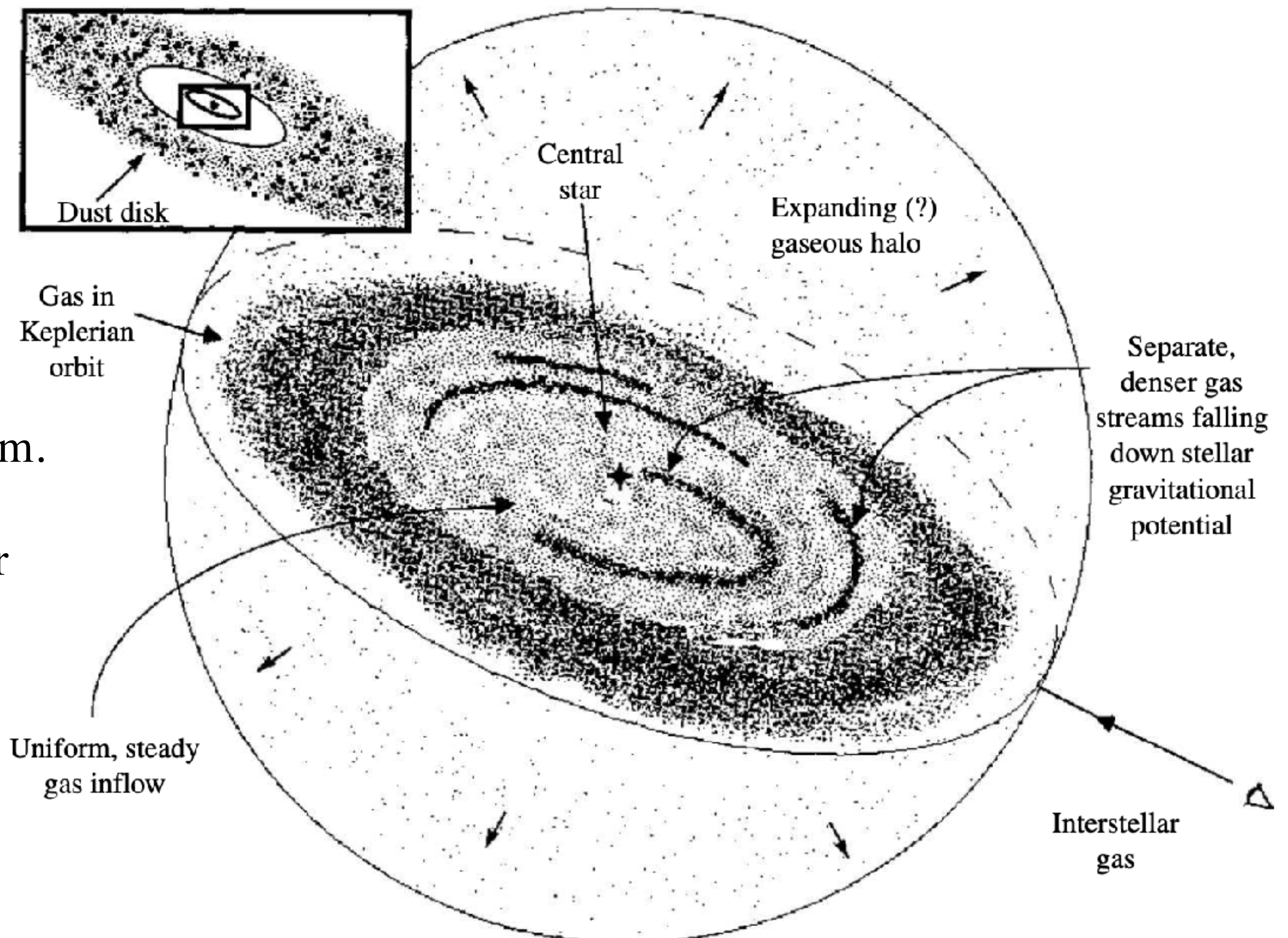
These disks may be **debris disks** rather than accretion disks, meaning that the observed material is due to collisions between objects already formed in the disks.

Hubble images also show a **secondary dust disk**, which may point to a planet formed on an inclined orbit.



Young stars with circumstellar disks

An artist's conception of the β Pictoris system. Clumps of material appear to be falling into the star at the rate of two or three clumps per week. Some matter may also be leaving the system as an expanding halo.



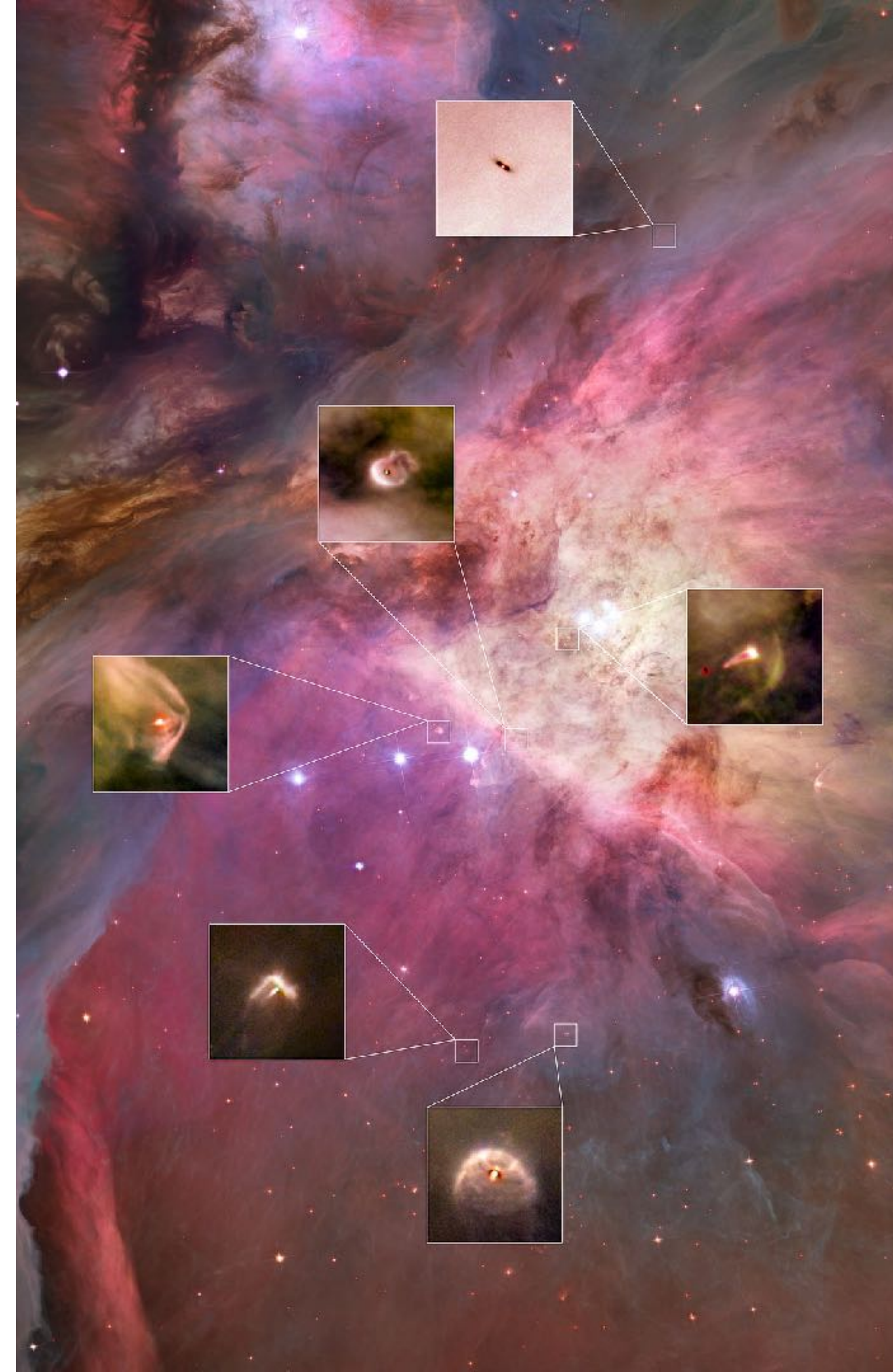
Proplyds

In 1993 the Hubble Space Telescope made observations of the Orion Nebula.

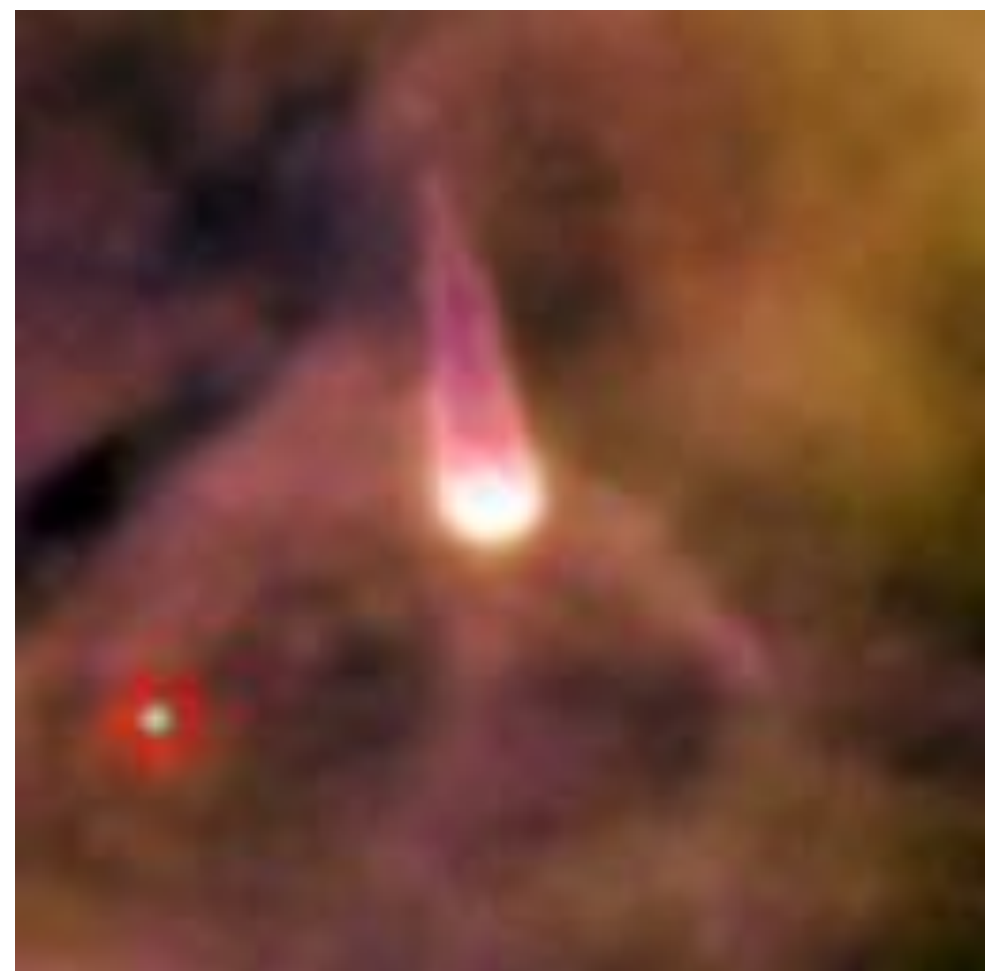
The images were obtained using the emission lines of H α , [N II], and [O III].

Analysis of the data has revealed that **56 of the 110 stars brighter than V =21 mag are surrounded by disks of circumstellar dust and gas**. The circumstellar disks, termed **proplyds**, appear to be **protoplanetary disks associated with young stars** that are less than 1 million years old.

Based on observations of the ionized material in the proplyds, the disks seem to have masses much greater than 2×10^{25} kg (for reference, the mass of Earth is 5.974×10^{24} kg).

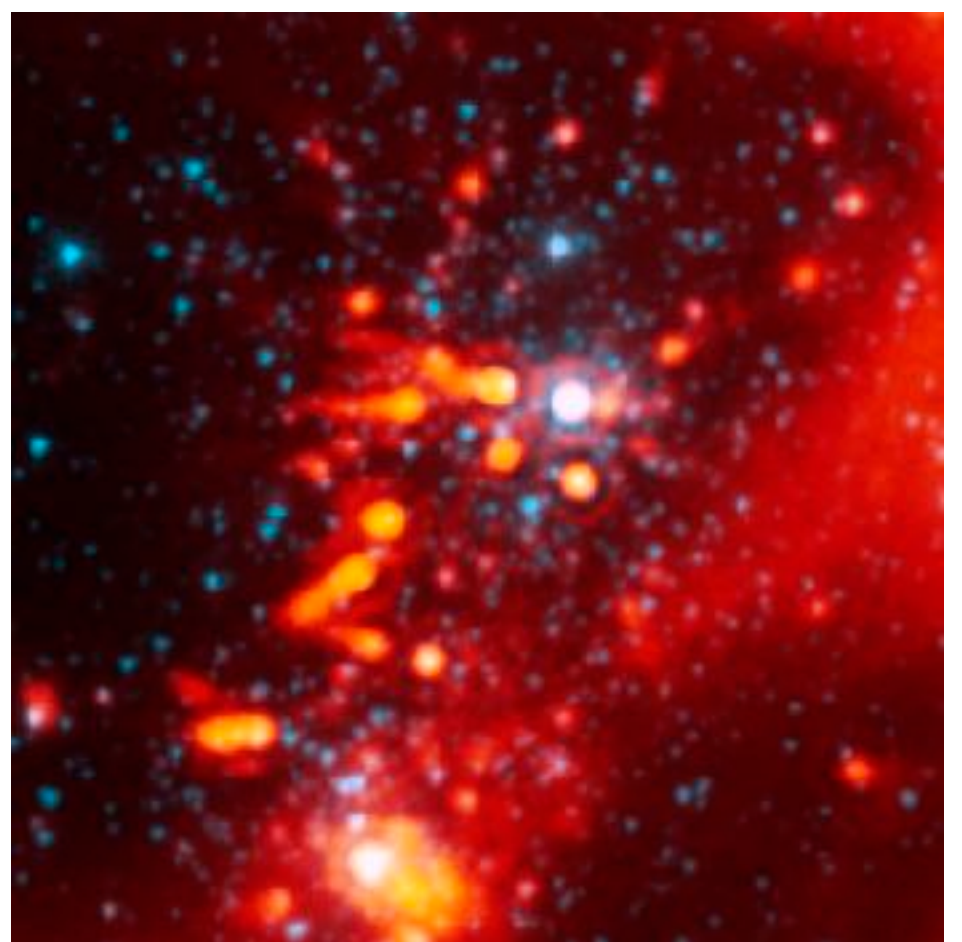


Proplyds



Harsh winds from extremely bright stars are blasting ultraviolet radiation at these stars and sculpting the gas and dust into its elongated shape.

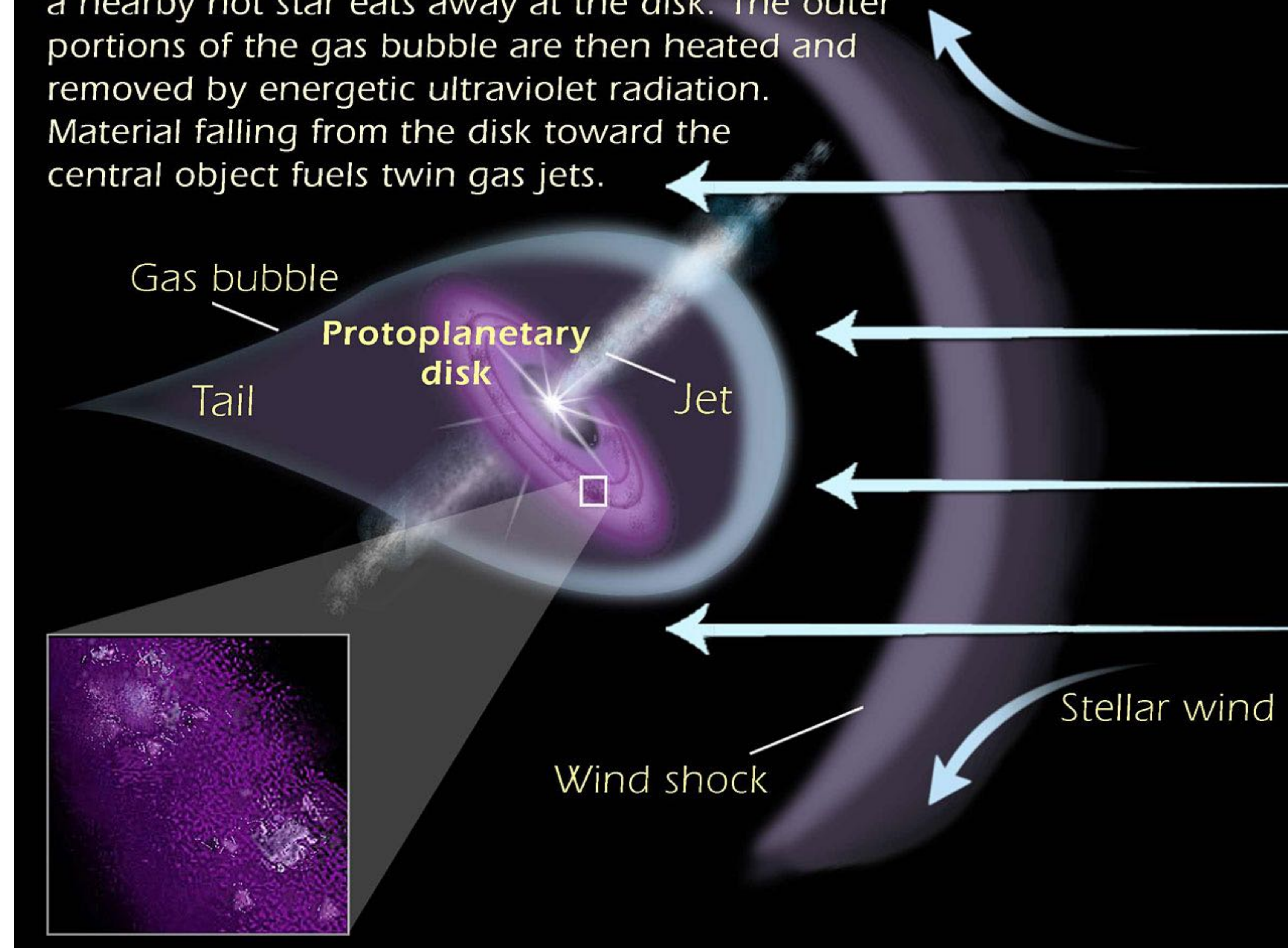
Proplyds



Proplyds observed
in infrared



As fine dust particles clump together deep inside the protoplanetary disk, ultraviolet radiation from a nearby hot star eats away at the disk. The outer portions of the gas bubble are then heated and removed by energetic ultraviolet radiation. Material falling from the disk toward the central object fuels twin gas jets.



Circumstellar disk formation

Disk formation is fairly common during the collapse of protostellar clouds.

Undoubtedly this is due to the **spin-up of the cloud as required by the conservation of angular momentum**.

As the radius of the protostar decreases, so does its moment of inertia. This implies that in the absence of external torques, the protostar's angular velocity must increase. By including a centripetal acceleration term and requiring conservation of angular momentum, the collapse perpendicular to the axis of rotation can be halted before the collapse along the axis, resulting in disk formation.

A **problem** immediately arises when the effect of angular momentum is included in the collapse. Conservation of angular momentum arguments lead us to **expect that all main sequence stars ought to be rotating very rapidly, at rates close to breakup**. However, observations show that this is **not generally the case**.

Apparently the **angular momentum is transferred away from the collapsing star**. One suggestion is that **magnetic fields**, anchored to convection zones within the stars and coupled to ionized stellar winds, **slow the rotation** by applying torques. Evidence in support of this idea exists in the form of apparent solar-like coronal activity in the outer atmospheres of many T Tauri stars.

Summary

